SHRP-C-677

Fiber-Optic Airmeter

Farhad Ansari

Civil and Environmental Engineering
New Jersey Institute of Technology

Strategic Highway Research Program
National Research Council
Washington, DC 1994

SHRP–C–677
Contract ID011
Product No. 4007

Program Manager: *Don M. Harriott*
Project Manager: *Inam Jawed*
Production Editor: *Marsha Barrett*
Program Area Secretary: *Carina Hreib*

January 1994

key words:
entrained air
fiber optic
fresh concrete
plastic concrete
reflected light intensity
volumetric method

Strategic Highway Research Program
National Academy of Sciences
2101 Constitution Avenue N.W.
Washington, DC 20418

(202) 334-3774

425/NAP/194

Acknowledgments

The research described herein was supported by the Strategic Highway Research Program (SHRP). SHRP is a unit of the National Research Council that was authorized by section 128 of the Surface Transportation and Uniform Relocation Assistance Act of 1987.

Contents

List of Figures

List of Tables

Abstract

This report discusses a three-phase program to evaluate both acrylate-filled and diamond-tipped air meter probes as well as to gather and evaluate test results comparing fiber optic measurements of entrained air in concrete mix to gravimetric and volumetric measuring methods.

The experiments indicate that while the acrylate-filled (plain-tipped) probes were effective in detecting the percentage of entrained air in the concrete mixes, the probes need to be altered to reduce the failure rate found during testing.

PROJECT SUMMARY

Quality control and condition analysis through nondestructive testing in concrete is one of the important issues addressed by SHRP research program. The objective of the research performed herein is to present a methodology for development of a test method and apparatus to determine the amount of entrained air void system in freshly mixed concrete to facilitate acceptance or rejection in the field.

The percentage of entrained air in freshly mixed concrete has been measured using the loss in light intensity outputs of thin Optical Fibers. Laboratory experiments were conducted for the development of a methodology. Reliability of results have been examined through experiments with air entrained concretes. The air content of concretes tested in this study ranged from 2 to 22 percent by volume. The fiber optic airmeter will be potentially useful in the determination of air void characteristics, particularly the distribution of entrained air system in freshly-mixed concretes. The consequences of the developed methodology will be the safeguard of concrete pavements against frost damage due to improperly air entrained mixtures, and therefore saving millions of dollars in highway rehabilitation costs.

INTRODUCTION

Deterioration of concrete structures due to freezing and thawing is one of the most significant problems of the concrete industry in northern climates. Some of the major problems in pavements such as scaling and spalling, popouts, D-line and pattern cracking are attributed to the deteriorating effects of temperature extremes on concrete. Degradation of concrete exposed to freezing and thawing is caused by a hydraulic pressure generated by the expansion of freezing water in the capillary cavities of concrete. The magnitude of the hydraulic pressure depends on the distance between capillary pores and an escape boundary, such as an air void. In concrete, disruptive stresses will be developed, unless every capillary cavity in the paste is not farther than three or four thousands of an inch from the nearest air void.

Ordinary concrete will contain a minimum of 1 percent of air voids. Experiments have indicated an expansion of 0.41 to 0.75 percent in concrete volume for a range of water to cement ratios at - 4 degrees Fahrenheit. Therefore, the amount of empty space in nearly all concrete is large enough to accomodate the extra volume required by freezing of water in the capillaries, but since the present empty space is not sufficiently near to all capillaries, frost action would deteriorate the concrete. This requirement can easily be met by the use of entrained air, which provides a fundamental solution to the problem of concrete deterioration due to freezing and thawing.

Air entrained concrete containing a large number of very small air bubbles is several times as resistance to frost action as non-air entrained concrete made of the same materials. Air entrained concrete should be a dense, impermeable mixture that is well placed, protected, finished, and cured if maximum durability is to be obtained. As it was mentioned earlier, the air voids are more effective when they are closer together, and the cement paste in concrete is normally protected against the effects of freezing and thawing if the spacing factor of the air void system is 0.008 in. or less as

determined in accordance with ASTM C 457. The air content and the size distribution of air voids produced in air entrained concrete are influenced by many factors, among the more important of which are:

1) The nature and concentration of the air entraining admixture.
2) Nature and proportions of the constituents of the concrete mixture.
3) Type and duration of mixing employed.
4) Consistency.
5) Kind and degree of compaction applied in placing the concrete.

Therefore, it is very important to control the quality of air entrained concrete during mixing, and placing.

MEASUREMENT OF ENTRAINED AIR IN CONCRETE

The percentage of entrained air in concrete must be carefully controlled since the freezing and thawing durability is impared if the concrete contains an insufficient amount of air, and strength is unnecessarily reduced if the percentage of air becomes excessive. The standard methods used to make air content determinations in freshly mixed concrete are the volumetric method (ASTM - C 137), gravimetric method (ASTM - C 138), and the pressure method (ASTM - C 231). For instance, in the Volumetric method a known volume of concrete is removed from the mix and mixed with water, agitating the mixture until the air separates from the slurry, and measuring the decrease in volume. In the Gaviometric method, the percentage of air is determined from the inverse relationship between the unit weight of concrete and the amount of entrained air. In the Pressure method, air which has been pumped to a predetermined pressure in a compartment of known volume is released into a sealed container full of concrete. The pressure volume relationship, Boyle's law, is then used to measure the amount of air.

Gravimetric method is basically a laboratory technique requiring careful measurements of unit weights of concrete constituents. This technique is not a method suitable for field applications. The volumetric method can be employed in the field, and it is capable of providing reliable results. However, it suffers from two major deficiencies in insitu applications. Firstly, depending on the operator's experience, it takes anywhere between 30 to 45 minutes to acquire reliable results using the volumetric device (Roll-A-Meter). Moreover, extraction of air from the concrete in a Roll-A-Meter requires intense agitation of the device which is dependent on the operator's strength. By employing the pressuremeter, an experienced operator is capable of measuring the air content of concrete in about 20 minutes. It is possible to come up with reliable results provided that the pressuremeter is well maitained and calibrated frequently.

None of the currently available technologies are considered to be rapid as far as applications to highway concretes are concerned. The desired device must be able to measure the air content of concrete rapidly (in a matter of seconds) so that the authorities will be able to make decisive actions during highway construction. It is also desirable to be able to measure the amount of entrained air at several locations in a pavement slab while it is being placed in order to assure uniformity of the mix

throughout the pavement. The system developed in this project offers the potential for being a superior technology for measuring air content, and eventual distribution of air void system in fresh concrete. It's application to highway concrete is currently hindered due to durability problems associated with the use of fiber optics in concrete. This report presents the current state of the fiber optic airmeter, experimental results, and suggestions for further research.

OBJECTIVES

Considering the importance of insitu monitoring of air content in freshly mixed concrete and it's future payoffs in construction of durable concrete highway pavements, a Fiber-Optic apparatus was developed at NJIT. The apparatus detects air bubbles in fresh concrete by measuring changes in the intensity of reflected light transmitted through a thin optical fiber that occur due to differences in the index of refraction between an air bubble and other constituents in concrete. A major component of the fiber optic probe is the sensor head which comes in contact with fresh concrete during measurement operations. The harsh enviroment in concrete tends to scratch and therefore damage the sensor head which is a quartz-based optical fiber. Therefore, it has been very difficult to obtain consistent measurements.

The primary objectives of the project described herein, consist of accomplishing the following tasks:

1. Fabrication of a hardened probe tip for the fiber optic airmeter.
2. Employment of the ruggedized probe in a series of experiments for verification of concepts developed earlier.

According to the terms of the contract, Research International was commissioned to fabricate the hardened probe tips and the opto-electronics module for the computer interface. NJIT employed the ruggedized version of the system in a series of tests involving: concretes, mortars, and mortars extracted from concrete. The air content for the materials tested ranged from 2.3 to 22 percent by volume.

SYSTEM COMPONENTS

As mentioned earlier, the main objective of the work reported here was the development and testing of a hardened probe head for the fiber optic airmeter. Research International was commissioned to prepare the probe tips and the peripheral instrumentation. In summary, Research International provided the following components of the hardware:

1. An Opto-electronic PC interface card for use with the fiber optic probe.

2. Operating software for testing operations and data logging.

3. Fabricated of plain tipped fiber optic probes. The plain tipped probes were strengthened by abrasion resistant ceramic pin ferrules. The ceramic pins were configured in a conical geometry to cover the periphery of the optical fiber. As shown in Fig.1, a number of probes were prepared in a

configuration where the tip of the fiber optic was flush with the ceramic housing. Another set of probe heads were prepared with a twelve micron deep pocket back filled with UV acrylyte. Ceramic housing cone angles were also altered to examine the effect of tip geometry on the sensor performance.

4. Refurbished the damaged sensors with a 2-day turn-around time. The letter suffix for the repeated serial number in table 1 indicates the number of times each sensor was repaired for further usage. For instance, the probe tip with serial number CO0001 was repaired two times. The new serial numbers for the repaired tip after each repair sequence are listed as CO0001B, and CO0001C in table 1 respectively.

5. Fabricated six diamond-tipped probes as indicated in table 1. The construction of diamond tipped probes resembled the acrylyte filled tips shown in Fig.1. However, instead of acrylyte, circular industrial grade diamond disks were epoxied to the optical fiber (Fig. 2).

6. Fabricated a hand-held vibrator for oscillating the probe.

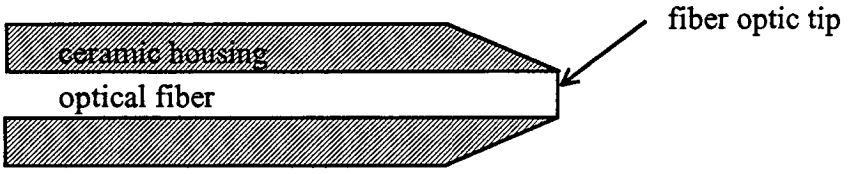

(a) fiber optic tip flush with ceramic

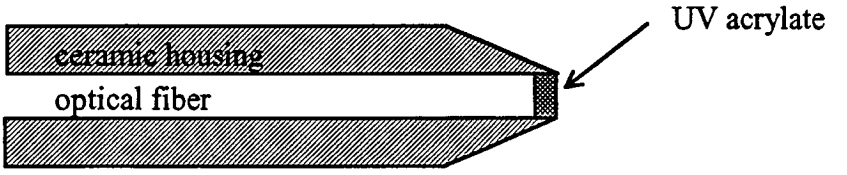

(b) 12 micron deep pocket back-filled with UV acrylate

Fig. 1 Plain-tipped fiber optic probe tip assemblies.

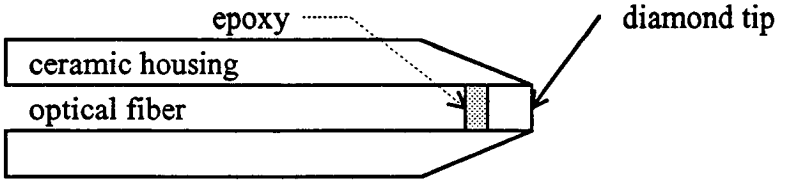

Fig.2 Diamond wafer probe tip.

Table I Air probe designation and description.

DATE	SERIAL NO.	CONE	FACE DIA.	TIP PREPARATION
08/26/92	CO0001	120°		Fiber tip flush with ceramic
	C00002	120°		Fiber tip flush with ceramic
	C00003	90°		Fiber tip flush with ceramic
	C00004	120°		Fiber tip flush with ceramic
	C00008	120°		12 μm deep pocket filled with UV acrylate
	CO0009	90°		12 μm deep pocket filled with UV acrylate
09/24/92	C00004 B	120°	0.65 mm	Fiber tip flush with ceramic
	C00008 B	120°	0.90 mm	12 μm deep pocket filled with UV acrylate
	CO0009 B	90°	0.55 mm	12 μm deep pocket filled with UV acrylate
	CO0010	90°	0.30 mm	Fiber tip flush with ceramic
09/25/92	CO0001 B	120°	0.45 mm	Fiber tip flush with ceramic
	C00002 B	120°	0.45 mm	Fiber tip flush with ceramic
10/08/92	C00002 C	120°	0.7 mm	Fiber tip flush with ceramic
10/27/92	CO0001 C	120°	0.6 mm	Fiber tip flush with ceramic
	C00002 D	120°	0.8 mm	Fiber tip flush with ceramic
	C00008 C	120°	0.90 mm	12 μm deep pocket backfilled with UV acrylate
	CO0010 B	90°	0.45 mm	Fiber tip flush with ceramic
	CO0009 B			Fiber cracked; not returned
	C00004 B			Ceramic pin broken off; not returned
11/4/92	CO0011	90°		Diamondcapped
	CO0012	90°		Diamondcapped
11/7/92	CO0013	90°		Diamondcapped, subsurface
	CO0014	90°		Diamondcapped, subsurface
11/12/92	CO0015	90°		Diamondcapped, subsurface

EVALUATION OF SENSOR TIPS

The sensor tips shown in figures 1 and 2 were evaluated through a series of preliminary experiments. It was not possible to evaluate the optical and signal detection capabilities of the diamond capped tips (Fig. 2) due to the detachment of the diamond disk from the tip assembly. The bond failure at the fiber to the diamond disk interface is attributed to the incompatability of the epoxy with the interface materials, namely the optical fiber and the diamond.

The UV acrylate-filled tips (Fig.1b) did not provide sufficient speed for the transmission of optical signals. Preliminary experiments with plain-tipped fibers (Fig.1a)indicated that they could be employed for testing concretes with water-cement ratios of 0.50 or higher, and largest aggregate size of 0.50 inches. These sensors showed good response for about ten repetitions in concretes so proportioned. In mortars, the same sensors exhibited excellent response for about twenty repetations. As it is demonstrated later, plain-tipped sensors provided sufficient optical response for detection of air bubble signals. These sensors are reparable, and most of them were re-polished and employed in experiments for about ten repetitions. It is also interesting to note that there was no need for using any aggregate repelling devices at the sensor tip. Aggregate repelling devices alter the flow characteristics of the concrete in the tip region. Our experiments indicated that a properly manufactured tip, even though made out of plain ordinary fiber, could withstand the harsh environment with no external aid from aggregate repelling devices.

Nominal aggregate diameters of one inch are typical in highway pavements, with water-cement ratios ranging from 0.35 to 0.45. Experiments with a typical highway mix indicated that none of these sensors could withstand the harsh environment in such mixes. Accordingly, the proof of concept experiments were implemented using the mix proportions given in the experimental section of this report. High air content concretes (i.e. 20% air) required more mixing water, and therefore, the mix proportions were dictated by the design air percent.

MEASUREMENT METHODOLOGY

Based on the foregoing discussions, plain-tipped sensors seemed to be the logical choice for further experimentation. Therefore, the experimental results presented in this report were acquired by employing the sensors shown in Fig. 1a. Acquired experimental data were processed through development of a set of mathematical algorithms, using MathCad. MathCad is an interactive computer software developed by Mathsoft, Inc..

As discussed in the previous reports, and shown in Fig.3, signal intensities at the interface between the optical fiber and any other medium such as fresh concrete are modulated according to the Snell's law. Refraction and reflection characteristics of transmitted light rays are governed by the refractive indices of the interface materials. The intensity of reflected signal is proportional to the square of the reflected amplitude according to the following relationship:

$$I = \left(\frac{n_1 - n_2}{n_1 + n_2}\right)^2 \quad \text{..... (1)}$$

where I is the reflected power density, n_1 and n_2 are the refractive indices of the optical fiber and the medium respectively.

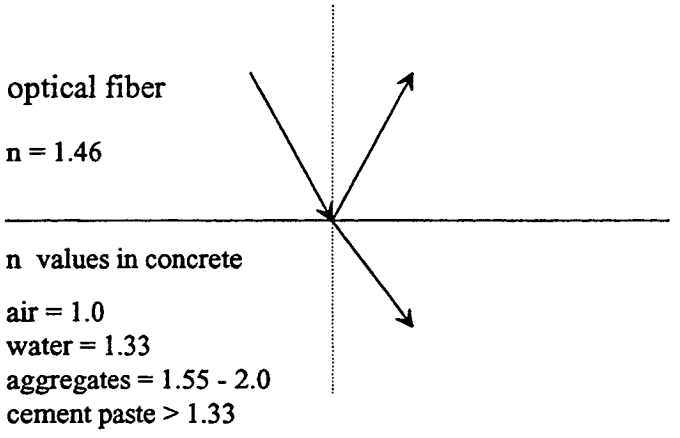

Fig. 3 Modulation of light intensity at the fiber to concrete interface according to the Snell's law.

As the sensor tip moves through fresh concrete, it comes in contact with concrete constituents including aggregates, paste, water, and air. Reflectivities conform to the refractive indices of constituent materials (Fig. 3), and are governed by eq. 1. A rough estimate of the percent reflectivities in fresh concrete can be made by using Eq. 1 as follows:

Reflectivity in air with n = 1 :

$$I = \left(\frac{1.00-1.46}{1.00+1.46}\right)^2 = 0.035 \approx 3.5\%$$

Reflectivity in cement paste, assuming it's refractive index equivalent to that of water, n = 1.33 :

$$I = \left(\frac{1.33-1.46}{1.33+1.46}\right)^2 = 0.0021 \approx 0.21\%$$

Relectivity using n = 1.56 for Mica to represent aggregate's response:

$$I = \left(\frac{1.56-1.46}{1.56+1.46}\right)^2 = 0.0014 \approx 0.14\%$$

As indicated above, signal levels are expected to be an order of magnitude larger in air when compared to other constituents. However, as shown in Fig. 4a, these computations pertain to situations where the surface area of the sensor tip is in full contact with a single constituent. The kinematics of relative motion between the sensor tip and individual constituents of varying dimensions in concrete during the motion of the sensor complicate the reflectivity pattern. As it is conceptually depicted in Fig. 4b, the surface area of the fiber tip during its motion in concrete will come in contact with a variety of consitutents.

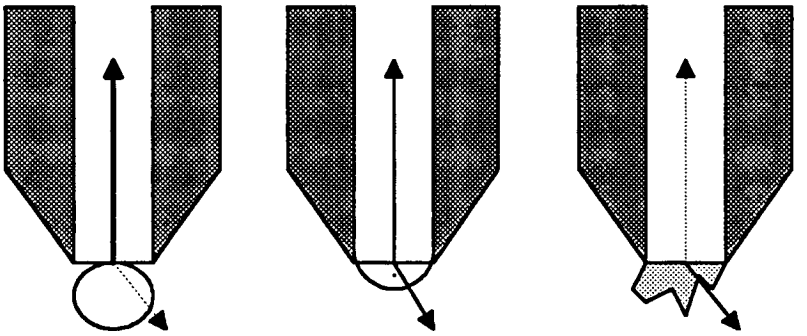

(a) fiber tip in full contact with a single constituent

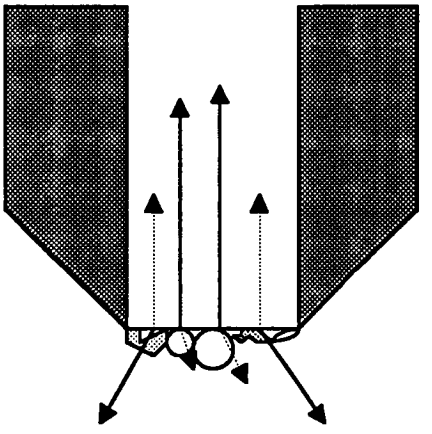

(b) realistic situation at fiber tip

Fig. 4 Conceptual diagram representing reflectivities at the fiber tip.

Reflectance due to air will depend on the area of sensor tip surface in contact with bubbles. Consequently, the amplitude of the reflected signal intensities will never

reach the maximum level shown in the computations. In spite of all the above-mentioned interferences, the intensity of reflected signals due to air bubbles are markedly larger than the ones due to other constituents. This is primarily due to the large difference in refractive index between an air bubble and other constituents in concrete. As the air content increases, so does the amplitude of signal corresponding to air. In other words, an increase in the density of air bubbles at the sensor tip is associated with a corresponding rise in the amplitude of the reflected signal (Fig.5

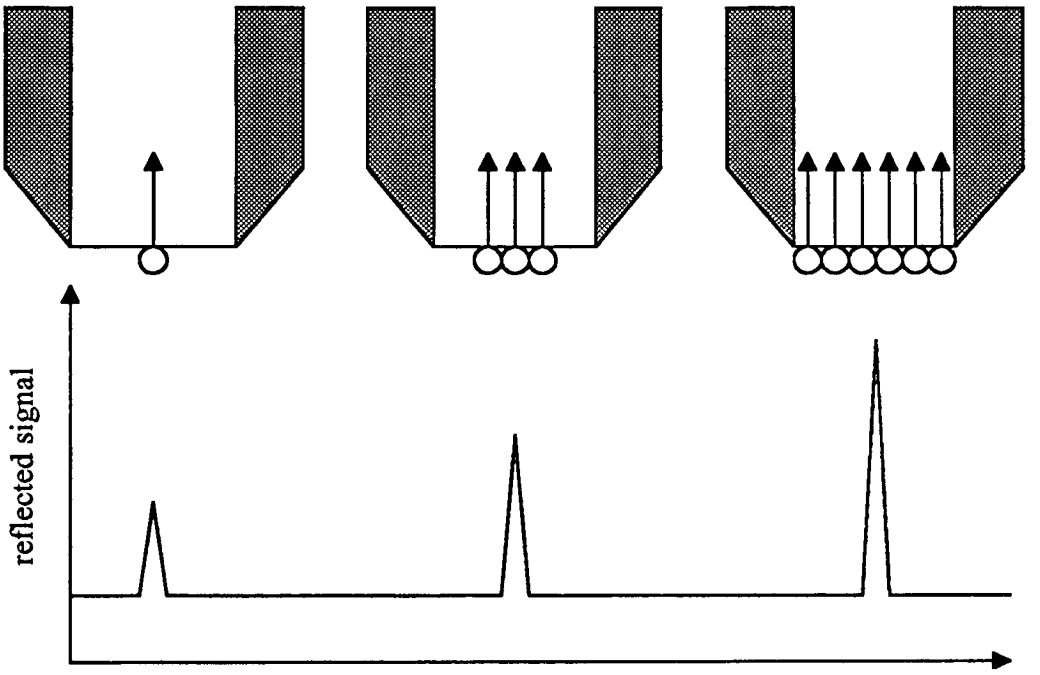

Fig.5 Correspondence between the signal amplitude and air bubble density at the fiber tip.

The amplitude of the reflected intensity is composed of low and high values corresponding to the refractive indices of the constituents. As mentioned earlier, air bubble signals are characteristically much larger than the reflected intensities associated with pastes and aggregates. Therefore, visual inspection of raw experimental data is hypothetically sufficient for recognizing signals due to air bubbles. As this works very well for concretes containing high air, detection of air bubbles in lower air concretes becomes more challenging. This is clearly demonstrated in Fig.5, since lesser number of air bubbles at the sensor tip result in lower amplitudes. An alternative method for detecting the lower amplitude, less noticeable air bubble signals from an experimental data is by forming a histogram plot. The histogram plot simply represents the frequency of data within the intensity spectrum. The abscissa in the histogram plot represents a sequence of intensity amplitude intervals given in ascending order. The ordinate gives the frequencies with

which the reflected intensities fall in the intervals. By inspecting the frequency plot, it is possible to find the threshold beyond which the intensity amplitudes correspond to the air bubbles. Raw experimental data representing signal intensities (in arbitrary units) as a function of data point number is shown in Fig.6. In reality, signal intensities are acquired as a function of time, with a total sensor run time of about twelve seconds. However, time intervals were converted to data numbers in order to save computer operation time during data file conversion routines. Fig.7 represents the histogram plot of data depicted in Fig. 6.

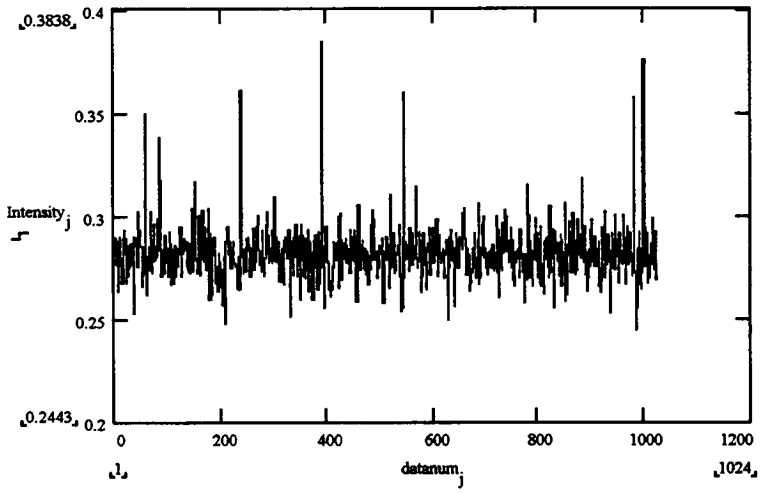

Fig. 6 Reflected intensity plot acquired from a typical experiment.

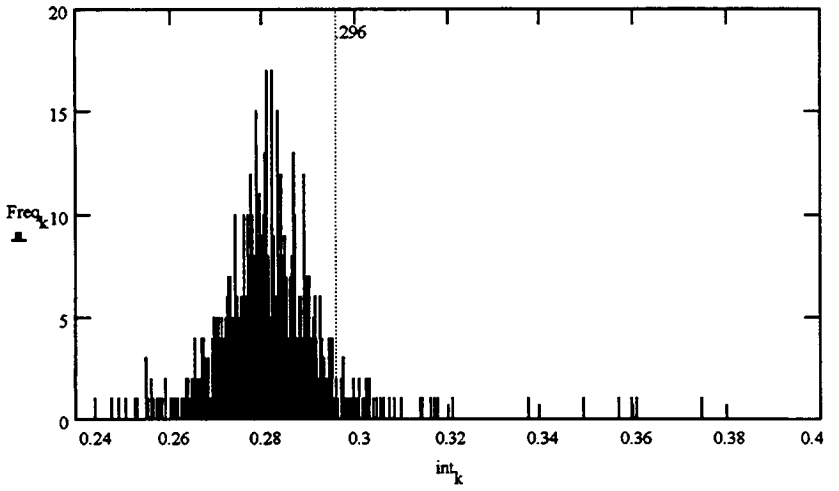

Fig. 7 Histogram plot representing the frequency of data at different signal intervals.

As the histogram in Fig.7 delineates, the signal intensity frequency plot resembles a normal distribution. Signal levels that correspond to concrete constituents other than air are tightly packed around the mean. Air bubble signal levels exhibit a marked increase in intensity as indicated by the gap in the frequency plot. The gap signifies the intensity threshold above which the signal levels correspond to air. As indicated in Fig. 7, for the data shown in Fig. 6, this threshold is at an intensity level of 0.297. Using the treshold level as the baseline for signal intensities it is possible to calculate percent air in concrete. Values above the baseline represent air , and values beneath it correspond to other constituents. In Fig.8, the baseline is shifted to the origin of the coordinates. Absolute signal values are measured with respect to the origin.

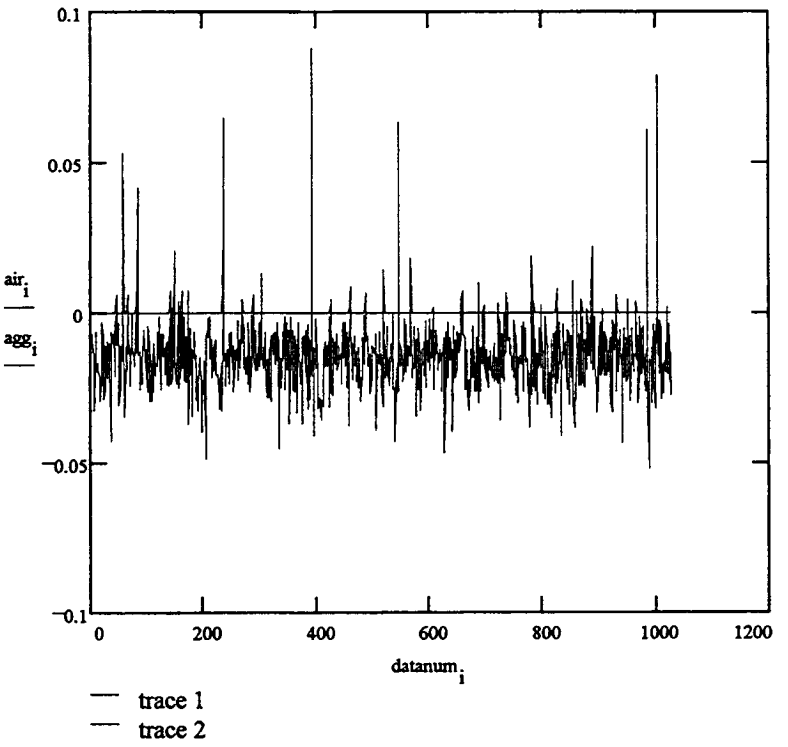

Fig. 8 Representation of reflected signal baseline at the origin of coordinates.

Computation of percent air in concrete is accomplished through the following steps:

1. summation of absolute signal levels above the baseline represent total air, and it is mathematically expressed as,

$$A = \sum a_i \qquad \text{.....(2)}$$

where a_i represent signal amplitudes corresponding to air, as shown by solid arrows in Fig.9.

2. signal levels below the baseline are summed according to the following relationship:

$$G = \Sigma g_i \quad \text{..... (3)}$$

where g_i represent signals corresponding to pastes and aggregates (dashed arrows in Fig. 9).

3. addition of Eqs. 2 and 3 gives the total value of signal generated in concrete:

$$T = A + G \quad \text{..... (4)}$$

4. percent air is calculated by:

$$air\% = \frac{A}{T} \quad \text{..... (5)}$$

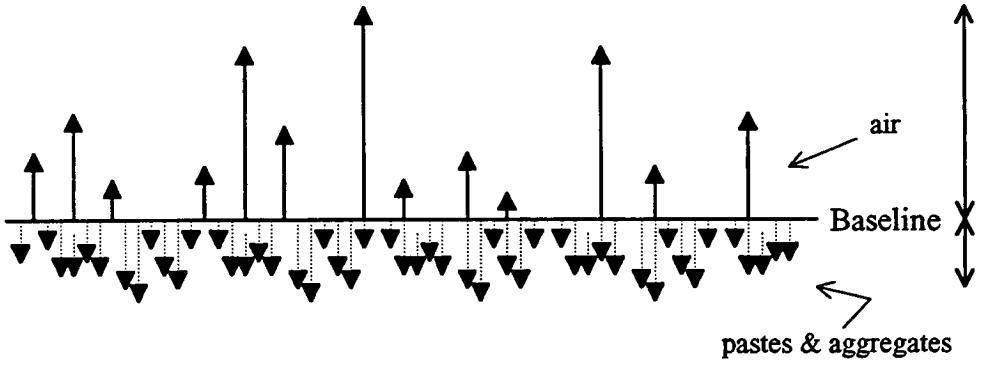

Fig. 9 Basis for calculation of percent air in concrete relative to the baseline.

The method described herein was employed for computing the air content of concrete using the fiber optic airmeter. Experimental details, measured air values, and discussion of results will be given in the following sections.

EXPERIMENTAL PROGRAM

The experimental program in this project consisted of three separate segments. During the early part of the work, the first phase of the experiments included those related to the evaluation of the sensor tips. These experiments were performed during the months of September and October, 1992. The experimental program during this phase of the project were not formalized. A variety of mix proportions were prepared for examining the ruggedness of the sensor tips, and the data acquisition parameters.

The experiments in phase two of the project were performed using the plain-tipped sensors. The objective during this phase of the project was to employ a single mix and vary the air content by progressively increasing the air entraining admixture. Data acquisition rate was set at 85 Hz, for a testing period of 12 seconds. Using these settings, it was possible to acquire 1024 points in each experimental run. Mix proportions for the concrete and mortar specimens tested in phase two of the project are given in tables 2 and 3 respectively. Type I portland cement conforming to ASTM C 150, ASTM No. 2 grade river sand passing through sieve No. 8, and maximum coarse aggregate size passing 0.375 inch and retained on No. 4 sieve were used. The air entraining agent employed in the present study was MBVR, a vinsol resin surfactant manufactured by Master Builders. Average mixing time for all the samples tested was between five to seven minutes. All phase two samples were mixed manually.

Table II Experimental program for phase 2 (concrete).

Date	Number of Experimental Runs with Fiber Optic Sensor	Mix Design by Wt.	Air-Entraining Admix. (milli-liter)	Air Content by P=Pressur-meter R=Roll-A-Meter
Nov. 19, 1992	8	1:2:2:0.55	0	4.0% (R)
Nov. 25, 1992	6	1:2:2:0.55	10	4.3% (R)
Dec. 02, 1992	2	1:2:2:0.55	20	5.4% (P)
Dec. 03, 1992	9	1:2:2:0.55	30	4.6% (P)
Dec. 04, 1992	1	1:2:2:0.55	40	6.5% (P)
Dec. 10, 1992	7	1:2:2:0.55	60	7.8% (P)
Dec. 11, 1992	4	1:2:2:0.55	80	7.8% (P)
Dec. 14, 1992	2	1:2:2:0.55	0	2.3% (p)
Dec. 15, 1992	5	1:2:2:0.55	0	2.3% (P)

Table III Experimental program for phase 2 (Mortar).

Date	Number of Experimental Runs with Fiber Optic Sensor	Mix Design by Wt.	Air-Entraining Admix. (milli-liter)	Air Content by P=Pressur-meter R=Roll-A-Meter
Dec. 23, 1992	3	1:2:0:0.50	30	7.50% (P)
Dec. 30, 1992	4	1:2:0:0.55	60	8.25% (P)
Jan. 08, 1993	5	1:1.9:0:0.55	60	9.90% (P)
Jan. 13, 1993	3	1:1.9:0:0.55	80	8.00% (P)

The experimental program in phase three consisted of more elaborate procedures for mixing and testing of specimens. These procedures involved: the development of a programatic method for developing concretes of very high air content; precise measurement of weights, volumes, and bulk densities of constituents employed in the mix for Gravimetric determination of air; and extraction of mortar from fresh concretes for further verification tests. To examine the effect of data acquisition rate on the experimental results, data acquisition rate was set at 340 Hz, for a testing period of 12 seconds. Using these settings, it was possible to acquire 4096 points in each experimental run.

Mixture Proportions

The ACI weight method[1] for mix proportioning of normal weight concretes was adopted for the mixes employed in the experiments. The ACI mix proportioning procedures employ charts and tables which relate the air content of air-entrained concrete to the amount of mixing water, and slump. Consequently, the amount of mixing water will influence the cement content, and the amount of sand used per cubic yard of concrete. The ACI recommended mix design tables are useful for mixing concretes of up to eight percent (8%) by volume air. However, our experimental program called for mixes containing air as high as twenty percent (20%). Therefore, prior to the verification tests, a mix proportioning trial and error procedure was employed for coming up with concretes of high air content ranging from ten to twenty percent. Using the ACI method as the first trial mix in a computer program (MathCad), it was possible to adjust the mixing water, and the sand content for the desired values. Although, in practice, the air contents of mixed concretes were not exactly similar to the simulated values, but it was possible to control the mix in such a way so as to obtain high air content mixes as desired. Mix proportions developed in this way were employed for mixing one cubic foot of concrete for each one of the verification tests performed in the laboratory. All the concretes were mixed

[1] Recommended Practice for Selecting and Proportioning for Normal Weight Concrete, ACI 211.1-70

in a rotary mixer, and mixing times were adjusted according to the desired air content. Mix proportions and experimental details are outlined in table 4.

Gravimetric Method for Air Content

ASTM test method C138, "Gravimetric Method for Measuring Air Content," was employed for measuring the air content as an alternate procedure. The specific gravities of fine aggregates were measured according to the ASTM, C128 test procedure. Computation steps were automated using the MathCad routines. Sample calculations are given in Appendix A. Measured air contents by the gravimetric method are given in table 4. Details regarding the laboratory measured values of concrete constituents and calculations pertaining to individual experiments are given in Appendix A.

Table IV Experimental program for phase three.

Date	No. of Runs with Fiber Optic Sensor in (concrete)	No. of Runs with Fiber Optic Sensor in (mortar)	Mix Design	Air -Entraining Admixture (milli-liter)	Air content in Concrete P=Pressure R=Roll G=Grav.	Air content in Mortar P=Pressure R=Roll G=Grav.
Feb. 12, 93	3	3	1:2.2:2.1:.55 0.75 cu.ft. of concrete	200	9.3% (P) 8.40% (G)	13.4% (R)
Feb. 19, 93	2	3	1:2.2:2.1:.55 1.0 cu ft of concrete	500	9.0% (P) 8.28% (G)	11.8% (P)
Mar 09, 93	2	4	1:3:1.35:.6 1.0 cu ft of concrete	150	22.0% (P) 16.88% (G)	17.0% (P)
Mar 23, 93	2	3	1:2.3:2.1:.58 1.0 cu ft of concrete	0	3.0% (P) 2.43% (G)	2.8% (R)
Apr 05, 93	4	4	1:2.3:2.1:.6 1.0 cu ft of concrete	30	11.5% (P) 9.07% (G)	13.0% (R)
Apr 07, 93	4	2	1:2.3:2.1:.6 1.0 cu ft of concrete	10	4.5% (P) 5.67% (G)	5.5% (R)

Sieved Mortar

The experimental program also involved testing the air content of mortars. However, the mortars tested during phase three of this research were extracted from the concretes through sieving operations (table 4).

The testing sequence involved mixing the concrete, measuring the air content simultaneously by the Fiber Optic and the pressure-meters (ASTM C231), extracting the mortar from the concrete, and measuring its air content using the Fiber optic, and either the pressuremeter or a Roll-A-Meter (ASTM, C173). Roll-A-Meter required less material for measurement, and therefore it was more suitable for testing the extracted mortar. The mortar extracting procedure involved passing the concretes through a No. 8 (2.36 mm) sieve. It was not possible to employ the Gravimetric method for measuring the air content of sieved mortar, since it was not possible to measure the mortar constituents apriori. Details pertaining to measurement procedures are outlined in Appendix A.

EXPERIMENTAL RESULTS

Experimental results representing the air contents of the materials tested during the entire course of this project are summarized in tables 5 thru 7. As indicated in these tables, in most cases, it was possible to run several fiber optic test runs in one experiment. In some cases, fibers damaged, and it was not possible to run more than few trials. This usually happened with the sensors that were already employed in prior experiments.

Table V Summary of results for concrete (phase II)

Date	No. of Runs by Fiber Optics	Air content by Fiber Optics for all runs per experiment (%)	Air content by other Methods (%) P=Press. R=Roll.
Nov. 19, 92	8	4.28, 4.5, 3.47, 3.34, 4.2, 4.49, 4.6, 3.36	R = 4.0
Nov. 25, 92	6	4.94, 3.81, 4.24, 3.88, 3.42, 3.89	R = 4.3
Dec. 02, 92	2	5.28, 5.51	P = 5.4
Dec. 03, 92	9	4.07, 5.0, 5.02, 4.68, 5.08, 4.53, 4.83, 3.96, 3.13	P = 4.6
Dec.04, 92	1	7.47	P = 6.5
Dec. 10, 92	7	7, 7.51, 9.8, 6.94, 6.74, 8.3, 6.6	P = 7.8
Dec. 11, 92	4	7.53, 9.11, 7.04, 7.4	P = 7.8
Dec. 14, 92	2	1.37, 2.9	P = 2.3
Dec. 15, 92	5	2.04, 2.8, 2.17, 2.33, 2.14	P = 2.3

Table VI Summary of results for mortar (Phase II)

Date	No. of Runs by Fiber Optics	Air content by Fiber Optics for all runs per experiment (%)	Air content by other Methods (%) P=Press. R=Roll.
Dec. 23, 92	3	6.6, 7.02, 6.4	P = 7.50
Dec. 30, 92	4	8.1, 7.6, 7.47, 8.9	P = 8.25
Jan. 08, 93	5	11.6, 11.2, 9.6, 11.8, 11.1	P = 9.90
Jan. 13, 93	3	11.87, 10.9, 12.7	P = 8.00

Table VII Summary of results in phase III

Date	No. of Runs by Fiber Optics in Concrete	No. of Runs by Fiber Optics in Mortar	Air Content in Concrete (%) F=Fiber Optics P=Pressuremeter R=Roll-A-Meter G=Gravimetric Method	Air Content in Mortar (%) F=Fiber Optics P=Pressuremeter R=Roll-A-Meter G=Gravimetric Method
Feb. 12, 93	3	3	P =9.3 G = 8.4 F =10.6, 9.77, 9.40	R = 13.4 F =13.16, 14.23, 12.5
Feb. 19, 93	2	3	P = 9 G = 8.2 F =10.4,8.78	P = 11.8 F =9.92, 10.80, 10.47
Mar. 09, 93	2	4	P = 22.0 G = 16.88 F =14.21, 15.20	P = 17.0 F =19.05, 22.5, 23.6, 19.48
Mar. 23, 93	2	3	P = 3.0 G = 2.43 F =2.40, 3.10	R =2.8 F =3.20, 2.47, 1.9
Apr. 05, 93	4	4	P =11.50 G = 9.07 F =10.47, 11.42, 12.18, 11.16	R =13.0 F =11.03, 14.5, 15.36, 14.92
Apr. 07, 93	4	2	P = 4.5 G = 5.67 F =5.10, 4.97, 4.53, 4.35	R =5.50 F =5.87

Fiber Optic data were analyzed according to the methodology described earlier (chapter I), and air contents presented in tables 5 thru 7 represent results from such analysis. Figs. 10 thru 34 depict raw data, and histogram plots for representative runs for all the experiments. As discussed earlier, these frequency distribution plots were employed in the detection of baselines for the air bubble signals. In the histogram representation of optical data, baselines are shown as dotted vertical lines. The signal intensity baseline values are displayed next to the dotted lines. In comparing the data presented in these figures, it should be noted that the plot axes were automatically scaled according to the signal levels. Therefore, attention should be given to the axes values for proper comparison. In these figures, measured air values are given in the legend.

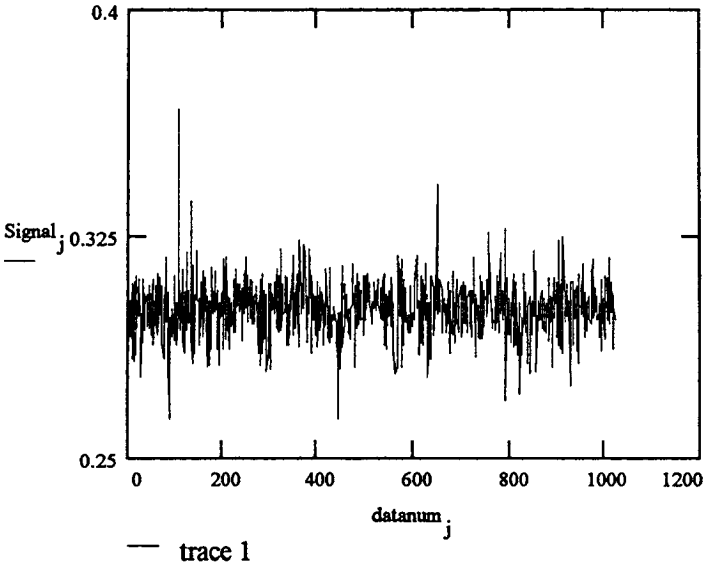

(a) Raw data representing the reflected signal intensity for 1024 data points.

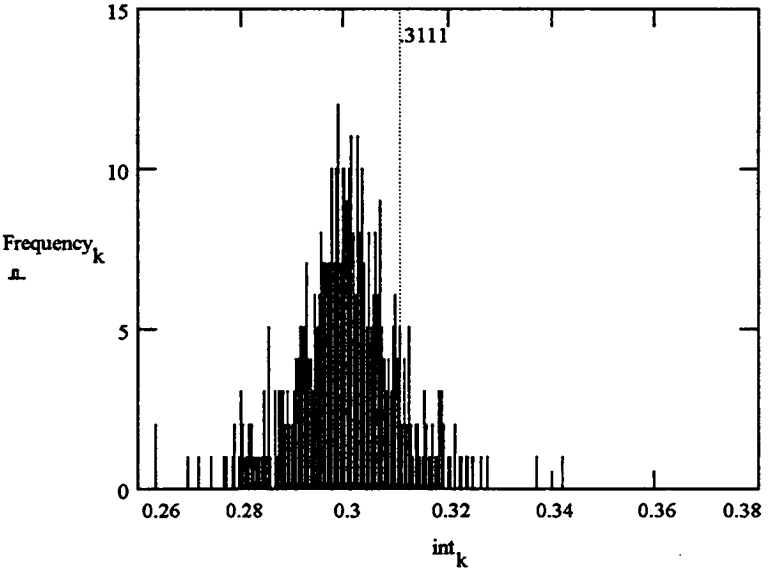

(b) Histogram plot of reflected signal intensities.

Fig. 10 Fiber Optic run results, data No. NOV19BA, F.O.=4.28%, R=4.0%.

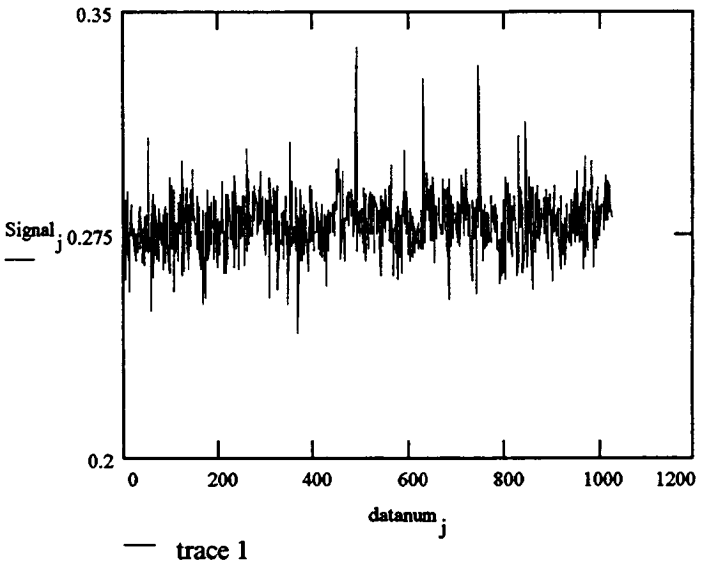

a) Raw data representing the reflected signal intensity for 1024 data points.

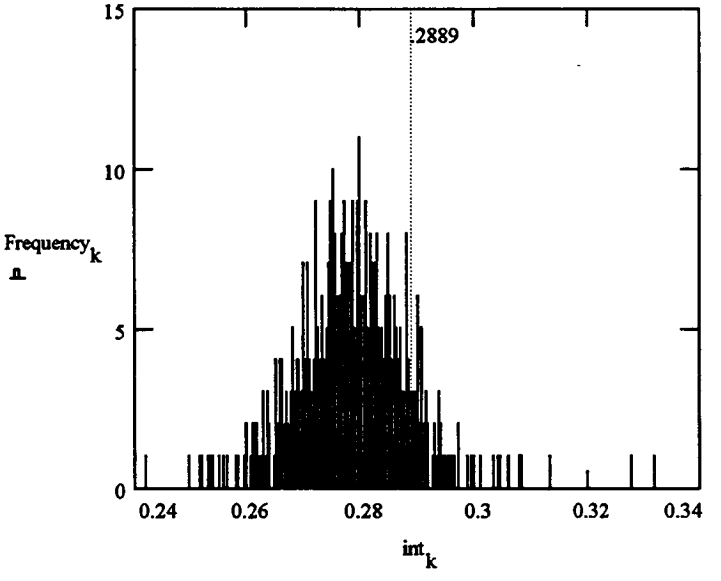

(b) Histogram plot of reflected signal intensities.

Fig. 11 Fiber Optic run results, data No. NOV25BA, F.O.=4.94%, R=4.3%.

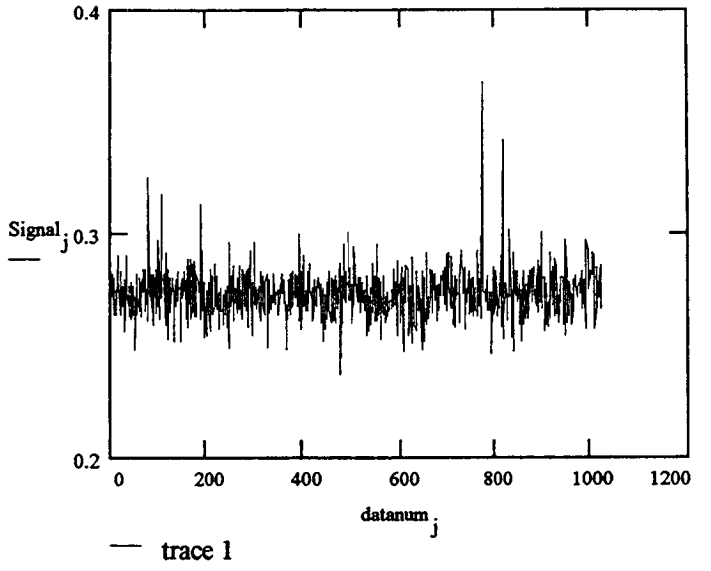

(a) Raw data representing the reflected signal intensity for 1024 data points.

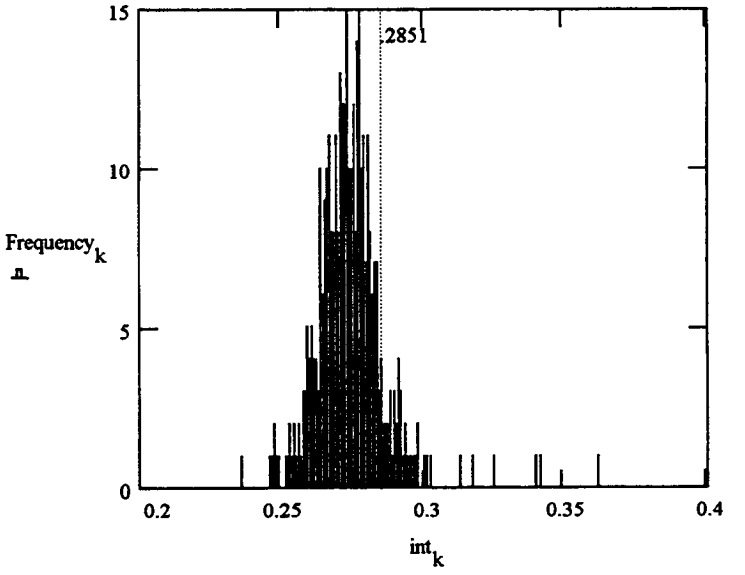

(b) Histogram plot of reflected signal intensities.

Fig. 12 Fiber Optic run results, data No. DEC02AE, F.O.=5.51%, P=5.4%.

(a)

(a)

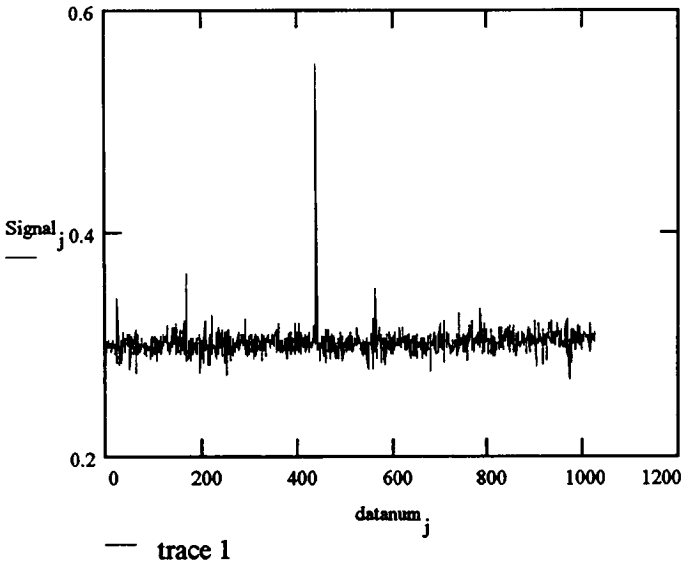

Raw data representing the reflected signal intensity for 1024 data points.

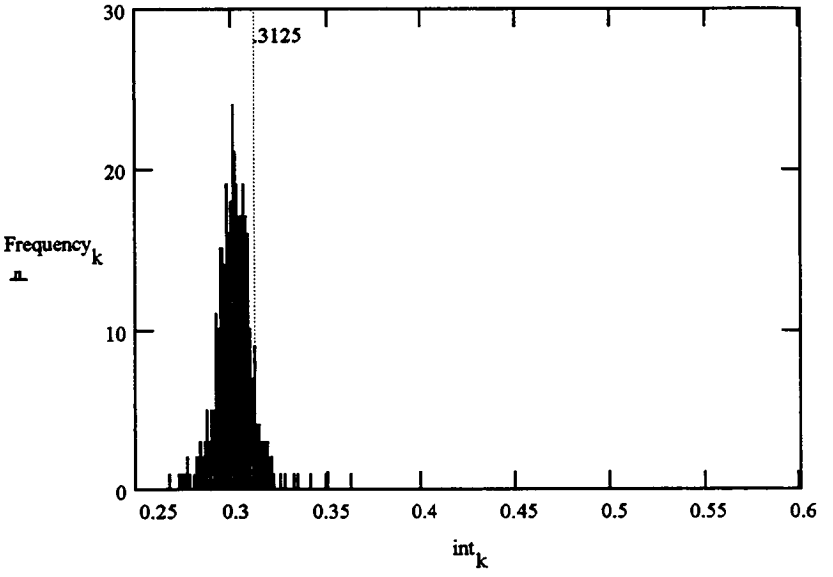

(b) Histogram plot of reflected signal intensities.

Fig. 13 Fiber Optic run results, data No. DEC03AD, F.O.=5.02%, P=4.6%.

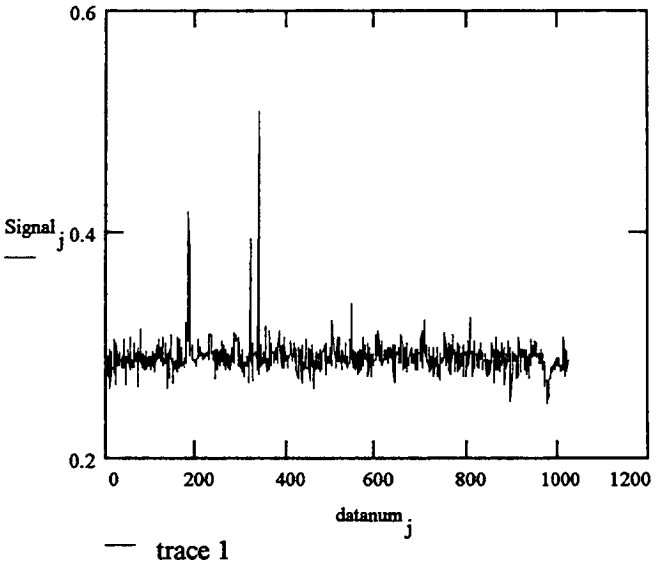

(a) Raw data representing the reflected intensity for 1024 data points.

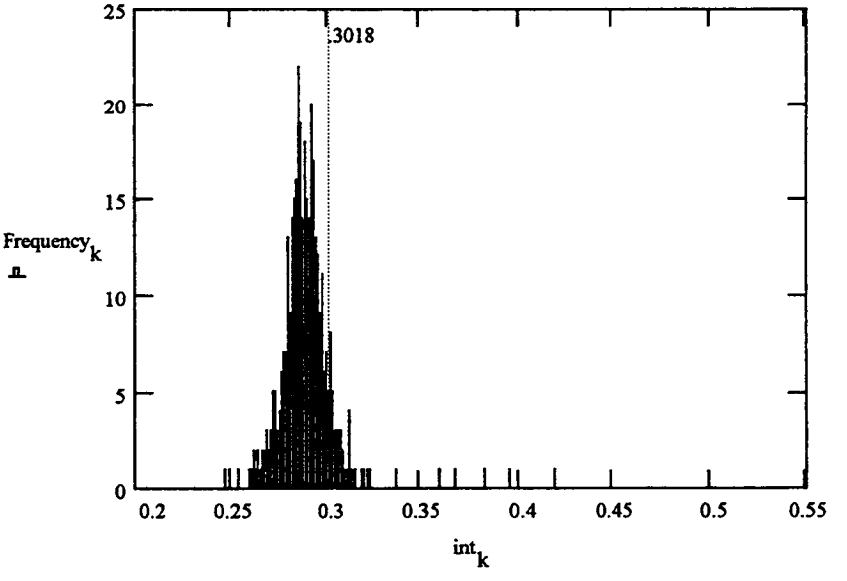

(b) Histogram plot of reflected signal intensities.

Fig. 14 Fiber Optic run results, data No. DEC04AA, F.O.=7.47%, P=6.5%.

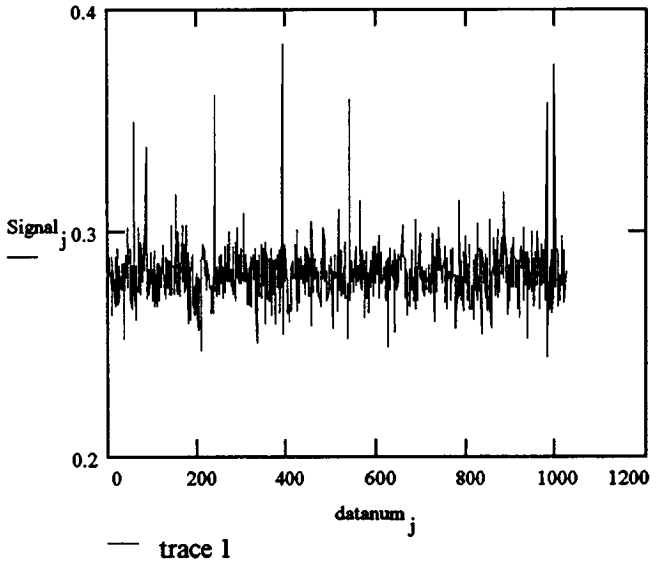

(a) Raw data representing the reflected intensity for 1024 points.

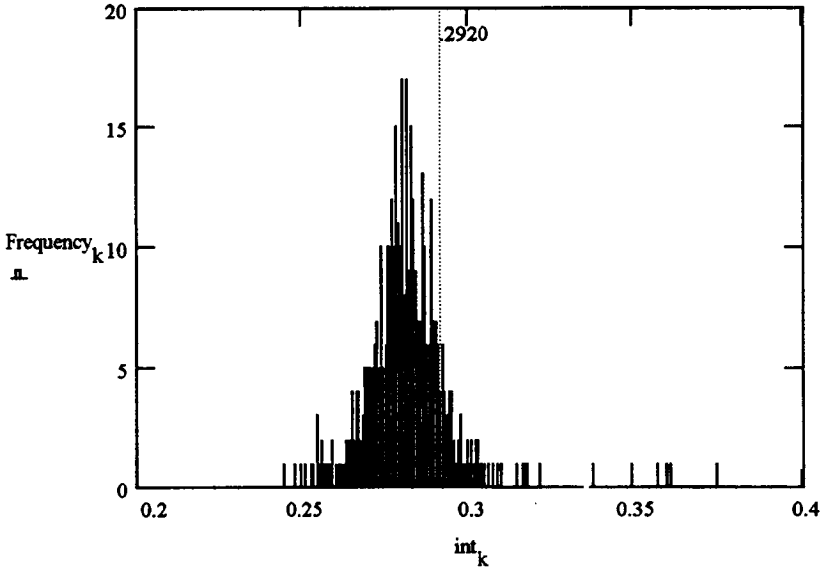

(b) Histogram plot of reflected signal intensities.

Fig. 15 Fiber Optic run results, data No. DEC10AF, F.O.=8.3%, P=7.8%.

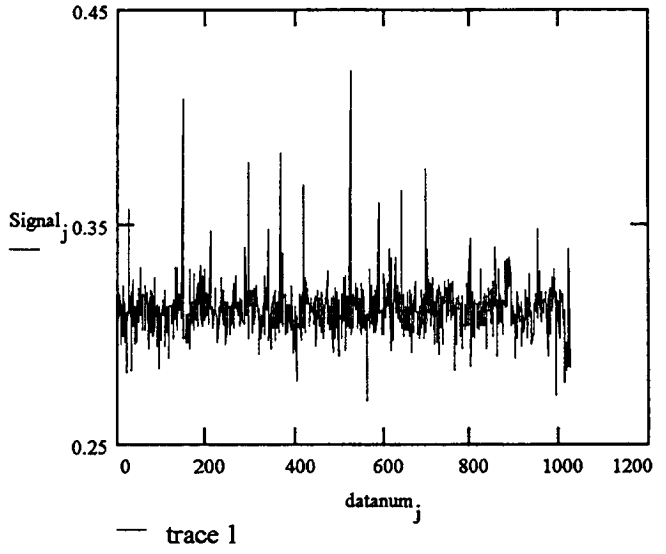

(a) Raw data representing the reflected intensity for 1024 points.

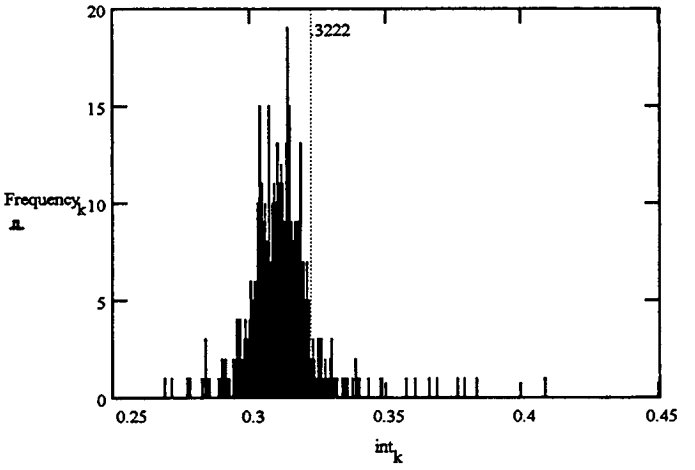

(b)

(b) Histogram plot of reflected signal intensities.

Fig. 16 Fiber Optic run results, data No. DEC11AA, F.O.=7.53%, P=7.8%.

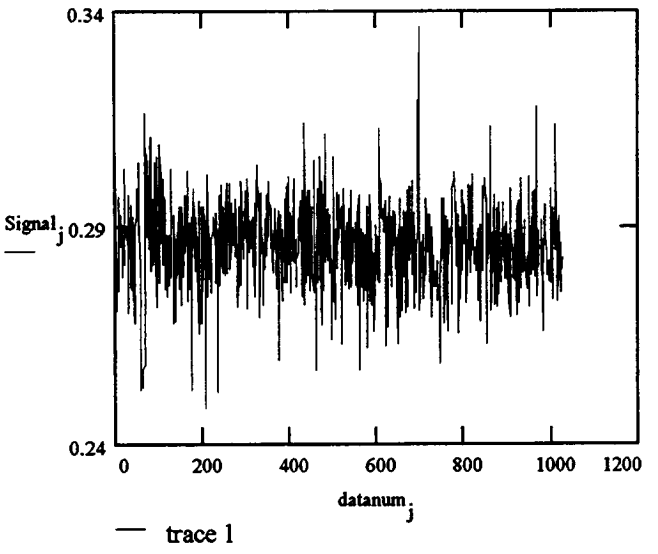

(a) Raw data representing the reflected intensity for 1024 data points.

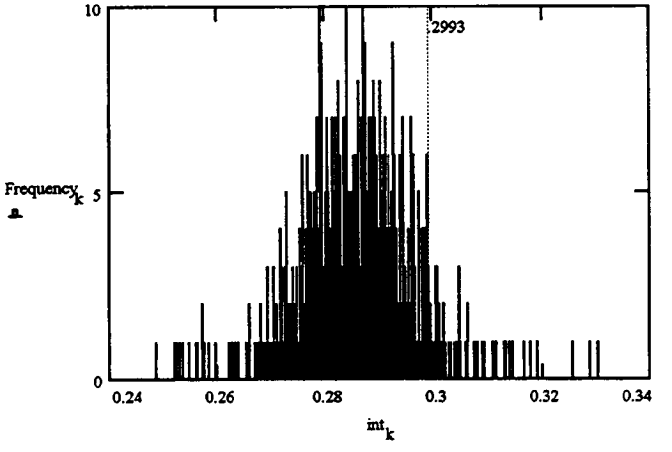

(b) Histogram plot of reflected signal intensities.

Fig. 17 Fiber Optic run results, data No. DEC14AE, F.O.=2.9%, P=2.3%.

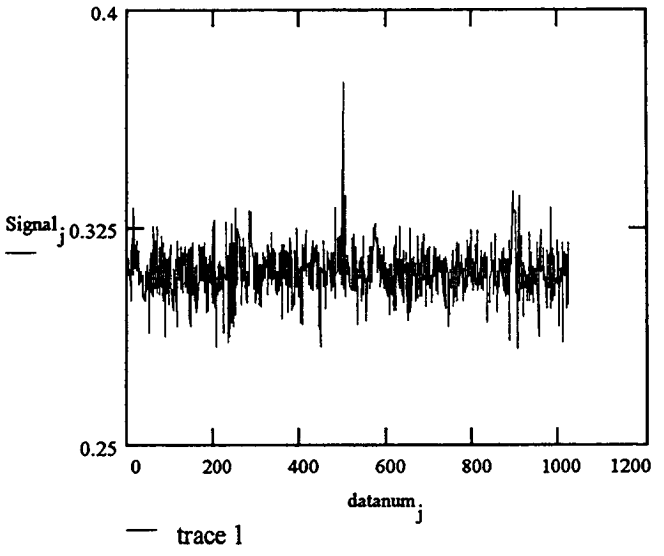

(a) Raw data representing the reflected intensity for 1024 data points.

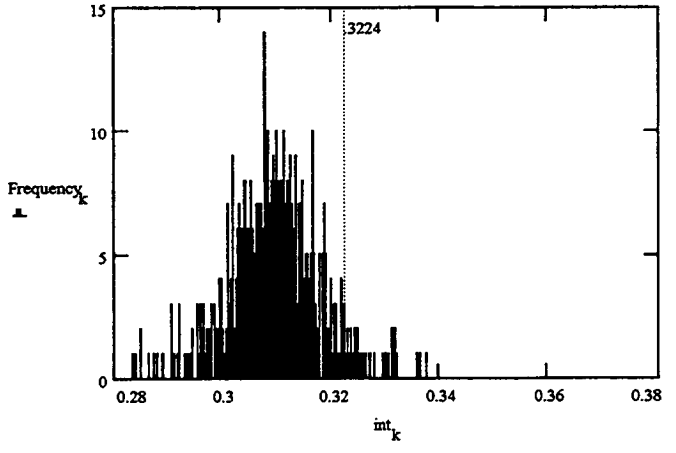

(b) Histogram plot of reflected signal intensities.

Fig. 18 Fiber Optic run results, data No. DEC15AG, F.O.=2.14%, P=2.3%.

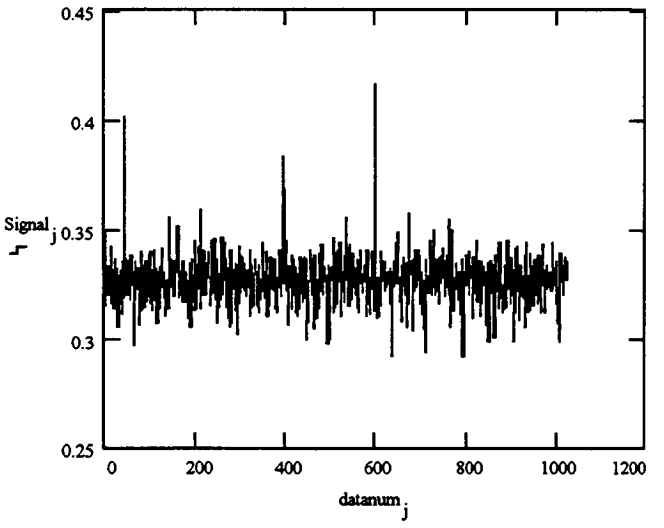

(a) Raw data representing the reflected intensity for 1024 data points in mortar.

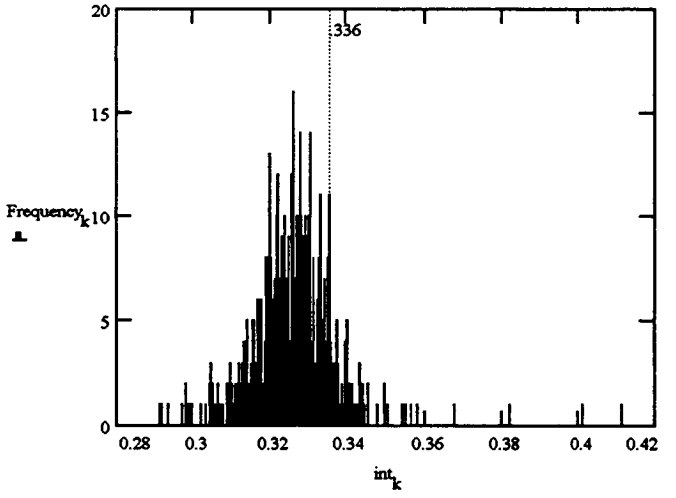

(b) Histogram plot of reflected signal intensities in mortar.

Fig. 19 Fiber Optic run results, data No. DEC23AB, F.O.=7.02%, P=7.50% (mortar).

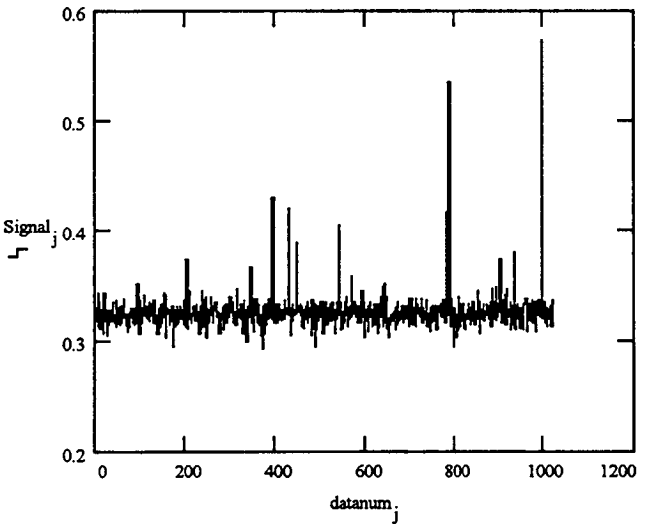

(a) Raw data representing the reflected intensity for 1024 data points in mortar

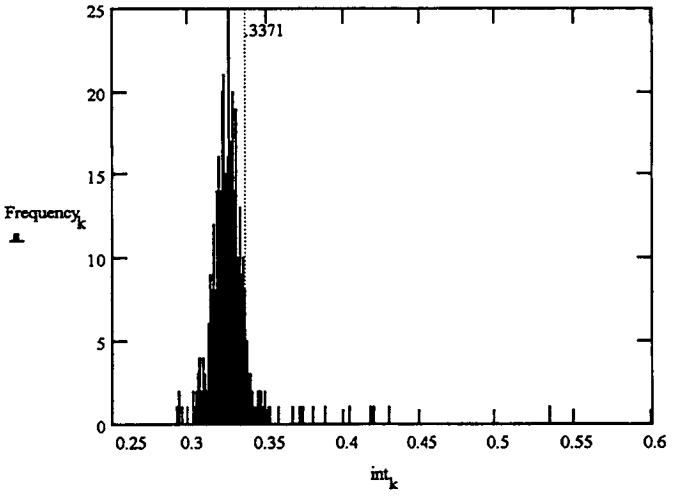

(b) Histogram plot of reflected signal intensities in mortar.

Fig. 20 Fiber Optic run results, data No. DEC30AD, F.O.=8.9%, P=8.25% (mortar).

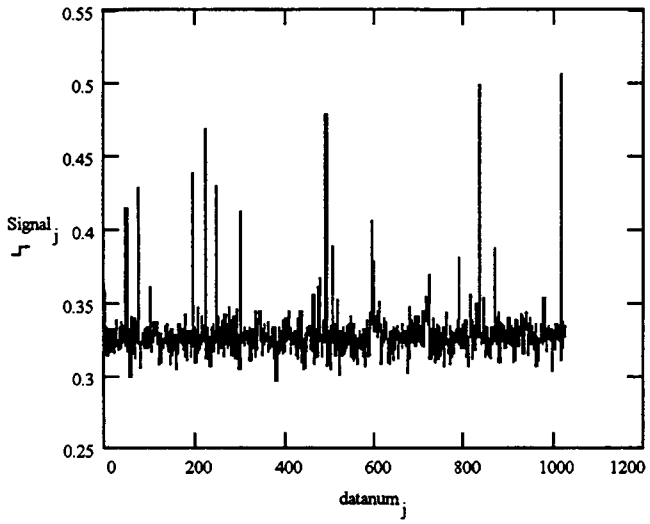

(a) Raw data representing the reflected intensity for 1024 data points in mortar.

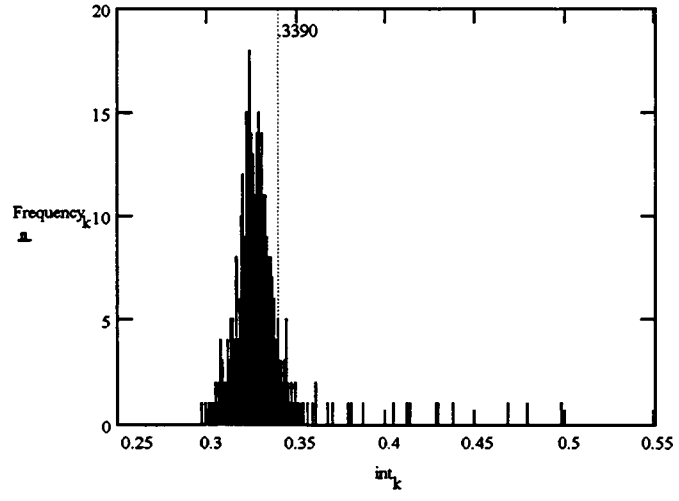

(b) Histogram plot of reflected signal intensities in mortar.

Fig. 21 Fiber Optic run results, data No. JAN08AE, F.O.=11.1%, P=9.90% (Mortar).

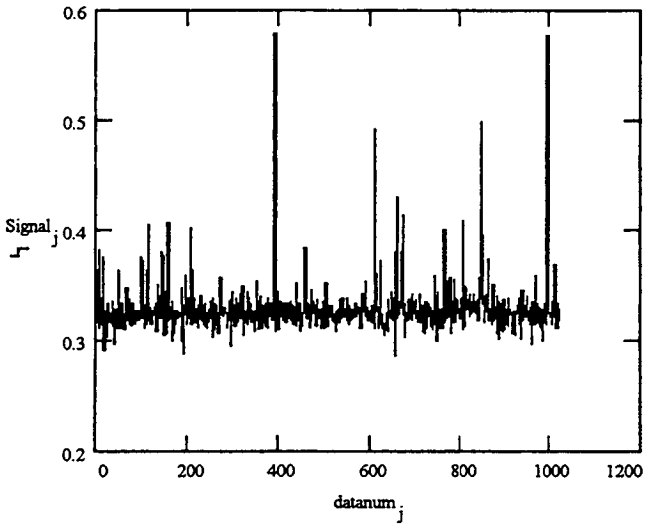

(a) Raw data representing the reflected intensity for 1024 data points.

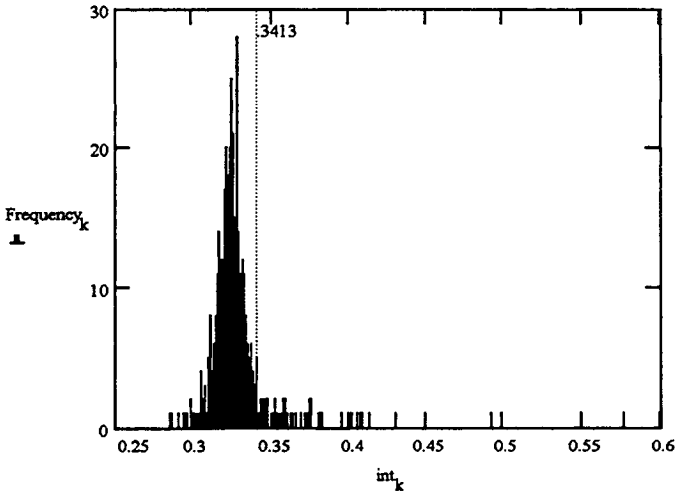

(b) Histogram plot of reflected signal intensities in mortar.

Fig. 22 Fiber Optic run results, data No. JAN13AD, F.O.=11.87%, P=8.00% (mortar).

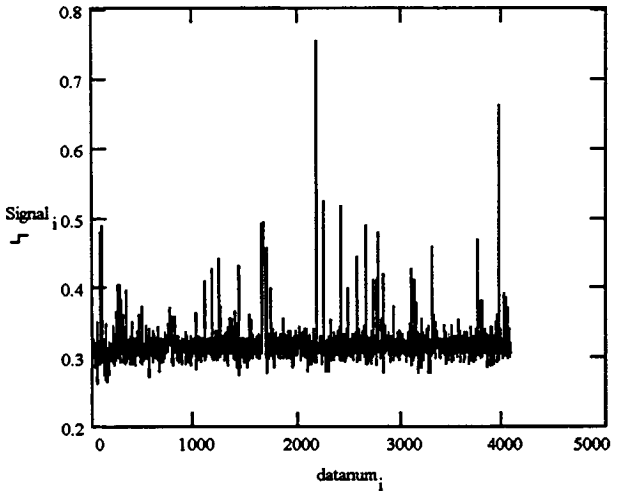

(a) Raw data representing the reflected intensity for 4096 points in concrete.

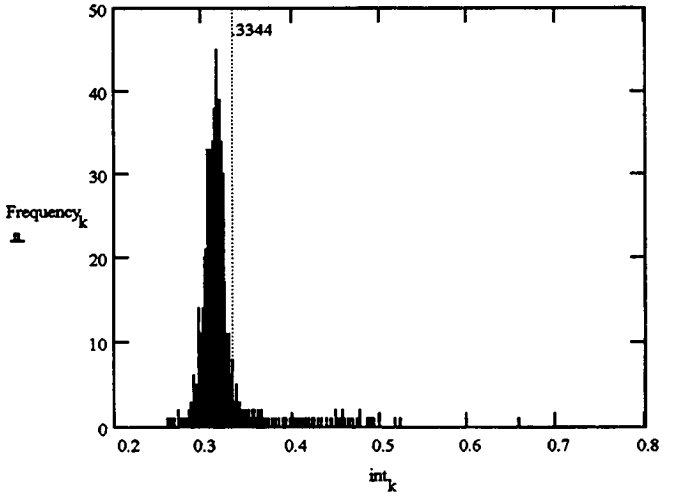

(b) Histogram plot of reflected signal intensities in concrete.

Fig. 23 Fiber Optic run results, data No. FEB12AE, F.O.=10.6%, P=9.3%, G=8.4% (Concrete).

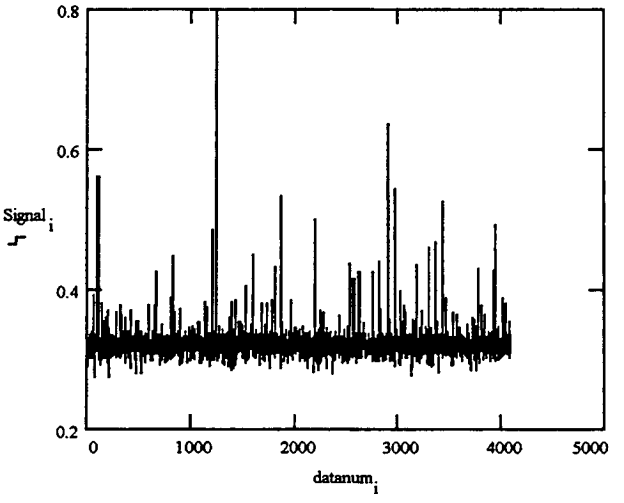

(a) Raw data representing the reflected intensity for 4096 points in concrete.

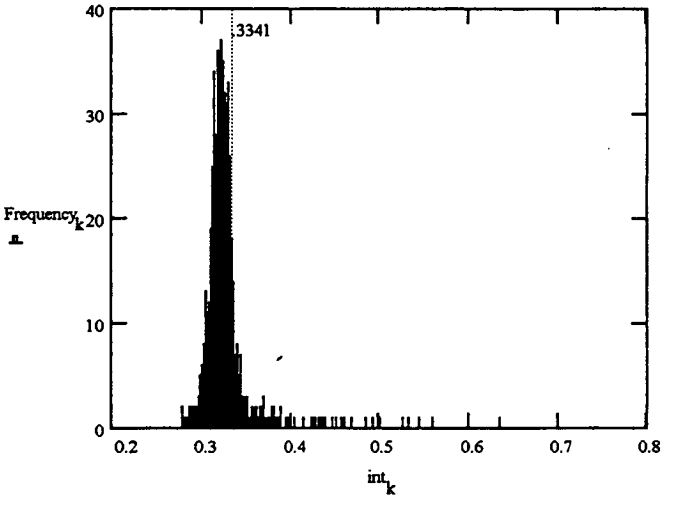

(b) Histogram plot of reflected signal intensities in concrete.

Fig. 24 Fiber Optic run results, data No. FEB12MD, F.O.=12.5%, R=13.4% (Sieved Mortar).

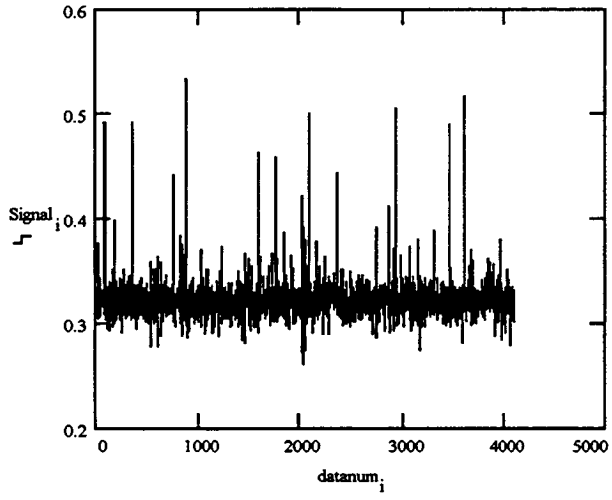

(a) Raw data representing the reflected intensity for 4096 points in concrete.

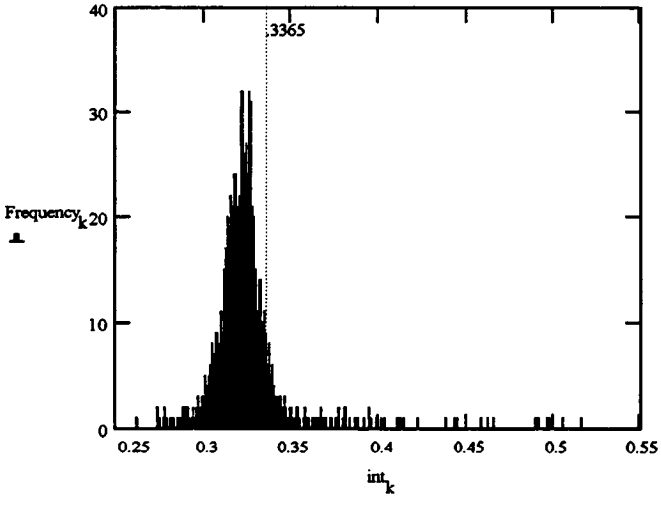

(b) Histogram plot of reflected signal intensities in concrete.

Fig. 25 Fiber Optic run results, data No. FEB19AC, F.O.=8.78%,P=9, G=8.2% (Concrete).

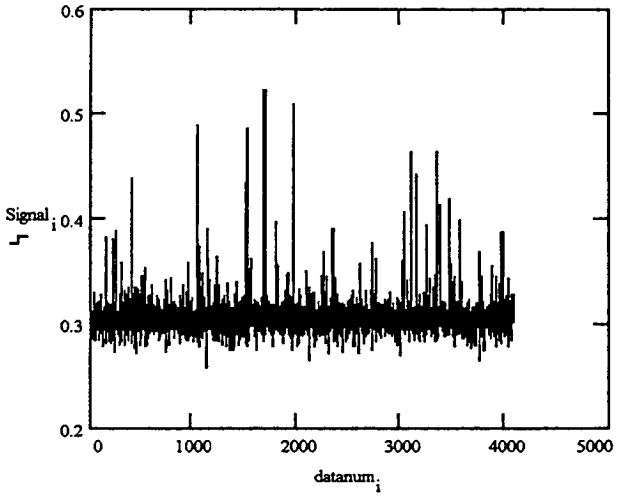

(a) Raw data representing the reflected intensity for 4096 points in concrete.

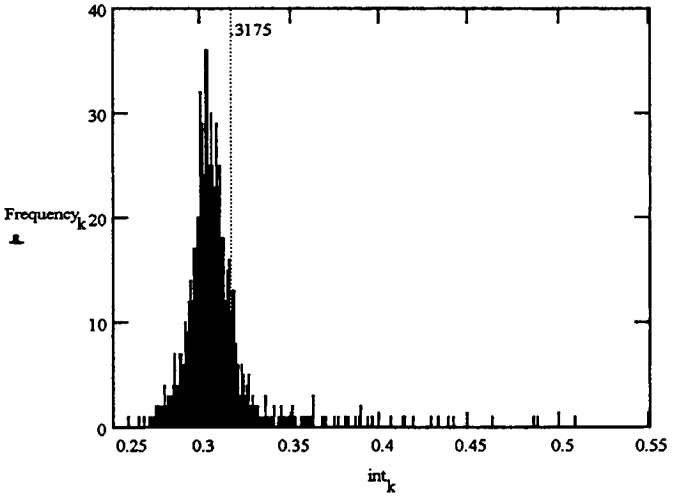

(b) Histogram plot of reflected signal intensities in concrete.

Fig. 26 Fiber Optic run results, data No. FEB19MC, F.O.=10.8%,P=11.8% (Sieved Mortar).

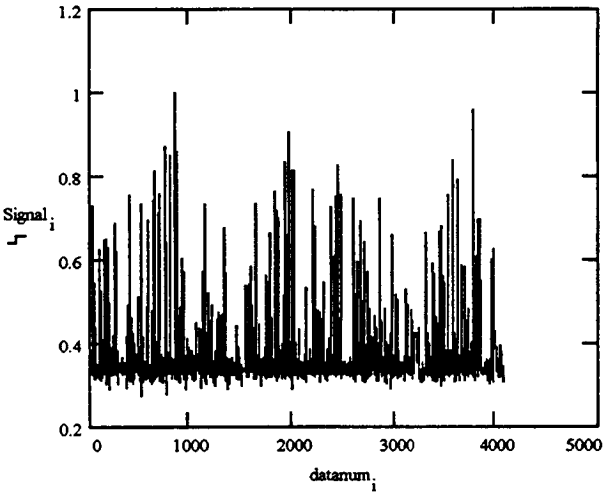

(a) Raw data representing the reflected intensity for 4096 points in concrete.

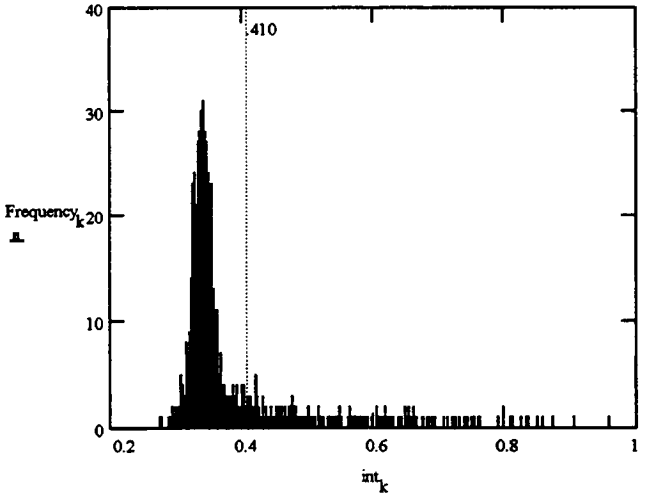

(b) Histogram plot of reflected signal intensities.

Fig. 27 Fiber Optic run results, data No. MAR09AB, F.O.=15.20%,P=22.0%, G=16.88% (Concrete).

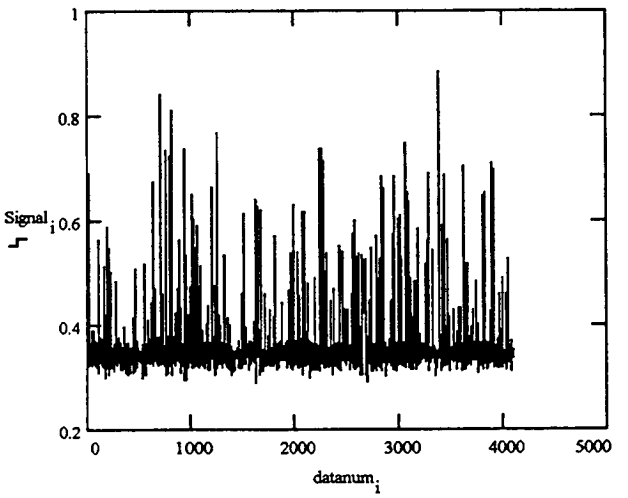

(a) Raw data representing the reflected intensity for 4096 points.

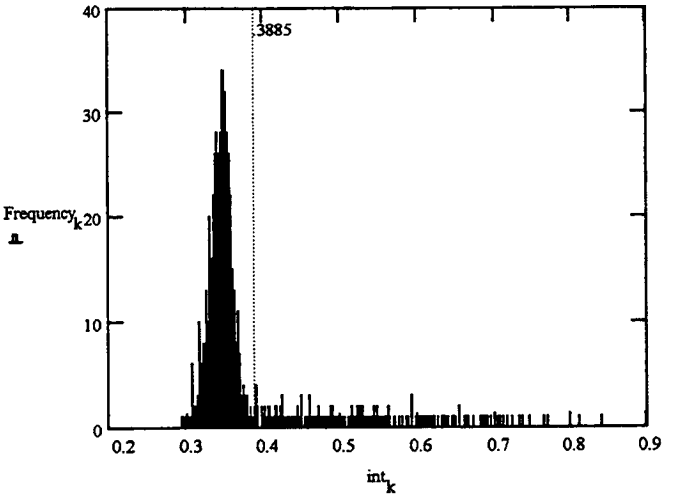

(b) Histogram plot of reflected signal intensities.

Fig. 28 Fiber Optic run results, data No. MAR09MA, F.O.=19.05%,P=17.0% (Sieved Mortar).

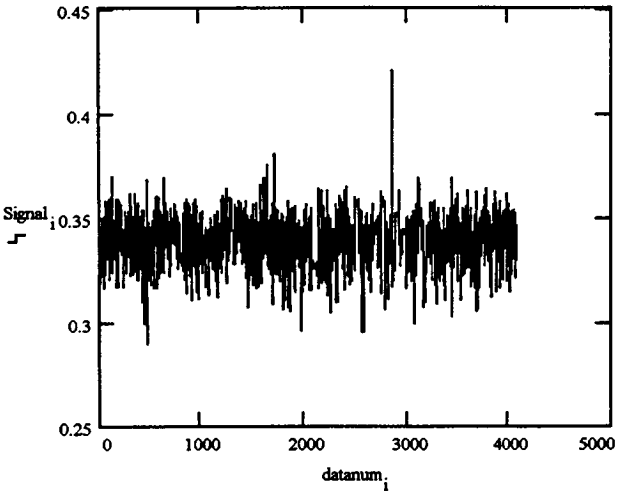

(a) Raw data representing the reflected intensity for 4096 points.

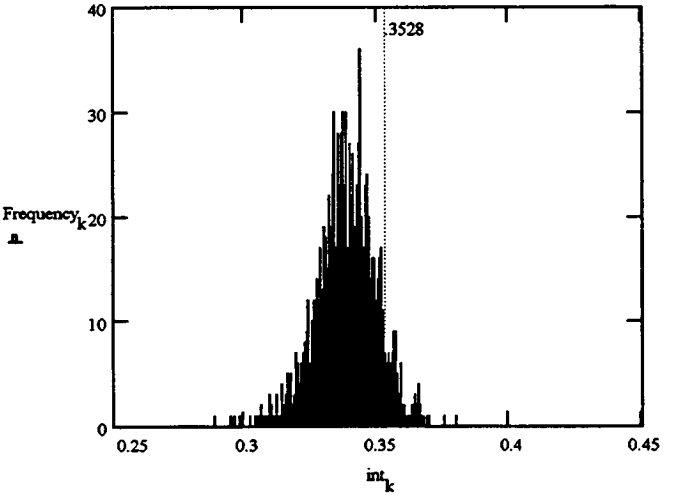

(b) Histogram plot of reflected signal intensities.

Fig. 29 Fiber Optic run results, data No. MAR23AB, F.O.=2.40%,P=3.0%, G=2.43% (Concrete).

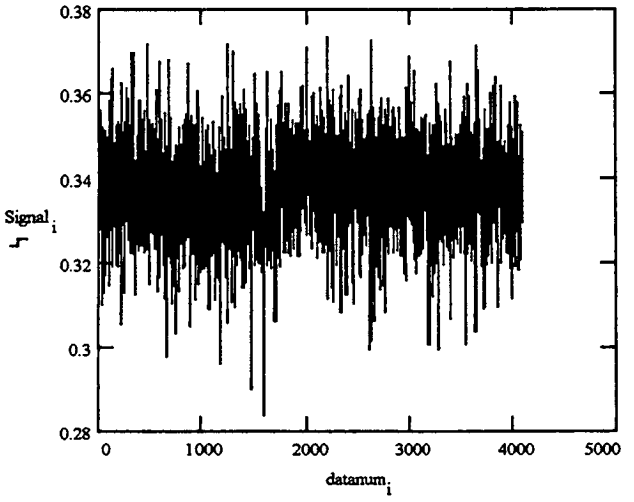

(a) Raw data representing the reflected intensity for 4096 points.

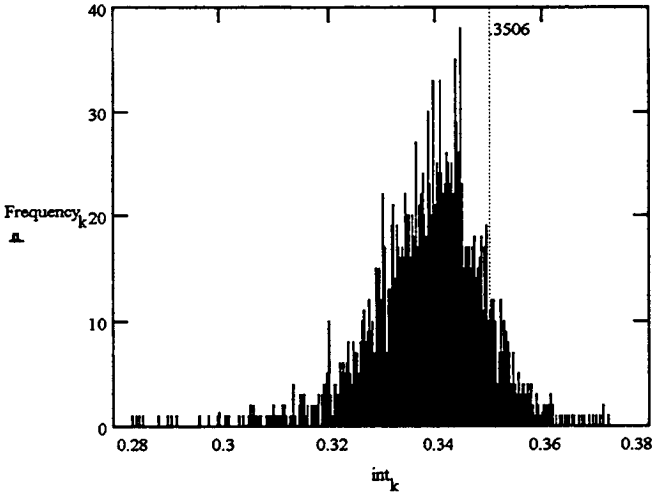

(b) Histogram plot of reflected signal intensities.

Fig. 30 Fiber Optic run results, data No. MAR23MB, F.O.=3.20%,R=2.80% (Sieved Mortar).

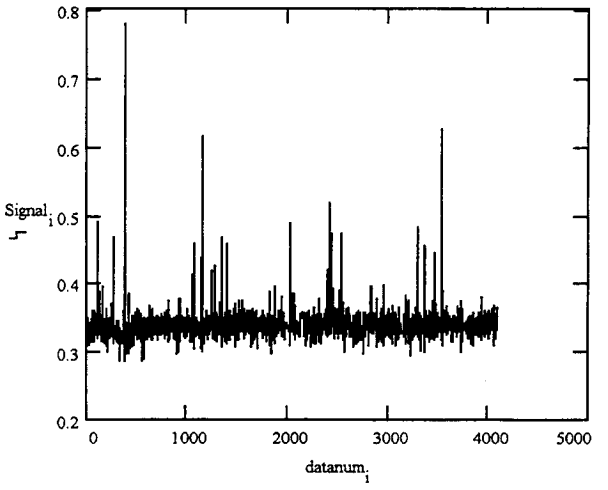

(a) Raw data representing the reflected intensity for 4096 points.

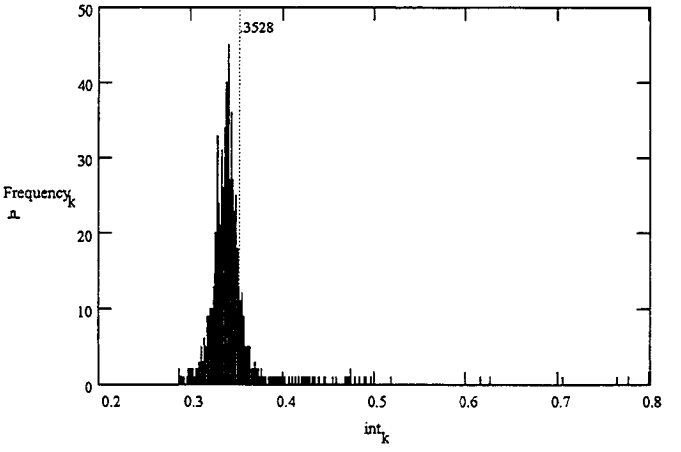

(b) Histogram plot of reflected signal intensities.

Fig. 31 Fiber Optic run results, data NO. APR05AB, F.O.=11.42, P=11.50, G=9.07, (Concrete).

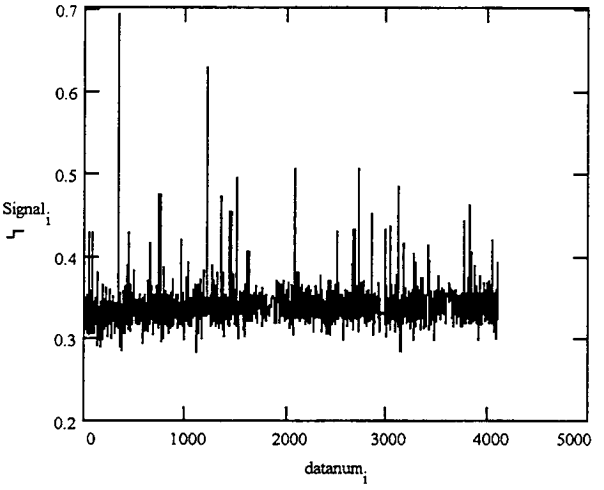

(a) Raw data representing the reflected intensity for 4096 points.

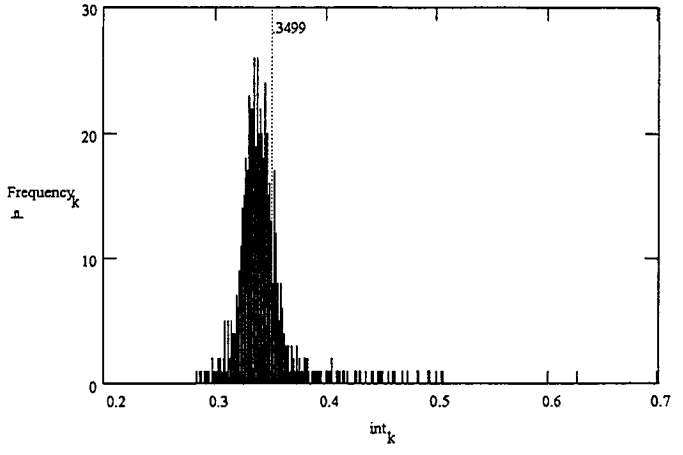

(b) Histogram plot of reflected signal intensities.

Fig. 32 Fiber Optic run results, data NO. APR05MC, F.O.=14.50, R=13.0, (Sieved Concrete).

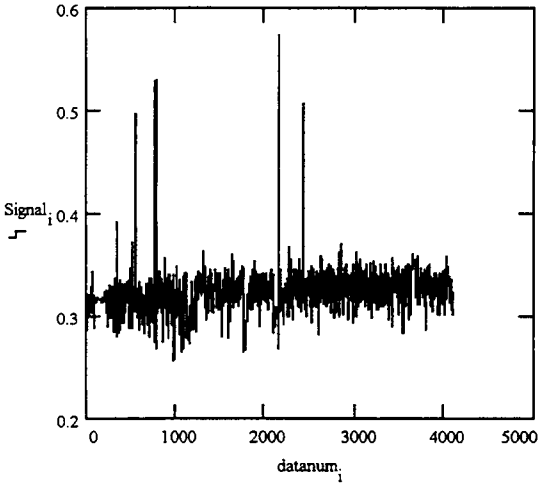

(a) Raw data representing the reflected intensity for 4096 points.

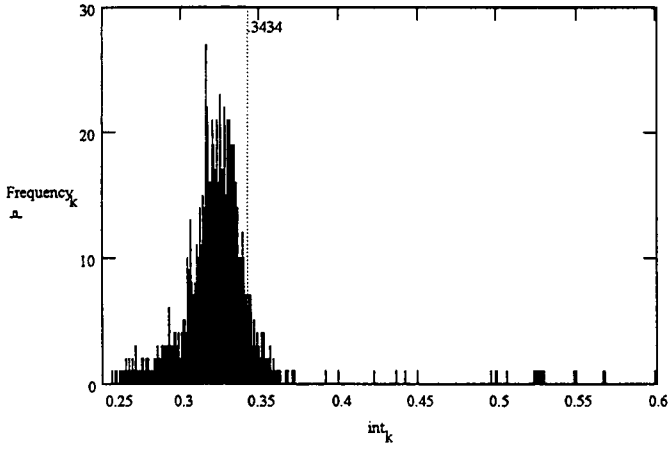

(b) Histogram plot of reflected signal intensities.

Fig.33 Fiber Optic run results, data NO. APR07AB, F.O.=5.10%, P=4.5%, G=5.67% (Concrete).

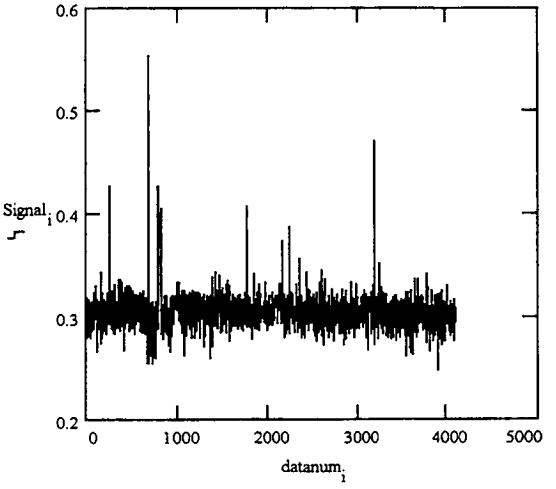

(a) Raw data representing the reflected intensity for 4096 points.

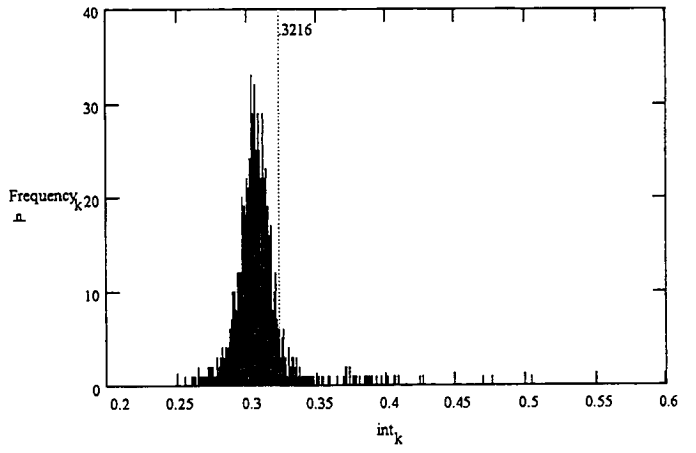

(b) Histogram plot of reflected signal intensities.

Fig.34 Fiber Optic run results, data NO. APR07MA, F.O.=5.87%, P=5.5% (Sieved Mortar).

DISCUSSION OF RESULTS

Figs. 35 and 36 present a comparison of air values measured by the optical fiber and the conventional methods (Pressure and Roll-A-Meters). These figures appertain to the experiments performed in phase 2 of the project. Measured air values for concrete using the fiber optics showed a good degree of correlation with the same using the conventional methods. However, for mortars tested on January 13, air values obtained by the optical fiber disagreed strongly with the ones acquired by using the pressuremeter. As indicated in table 2 of the experimental program section of this report, mix designs for mortars mixed on January 8, and 13 were identical except for the amount of air entraining admixture. The mortar mixed on January 13 contained 20 milli-liter more air-entraining admixture than the one mixed on January 8. Our objective for mixing the January 13 mortar was to obtain a mortar with higher air than the one previously tested on January 8. At this point, it is not clear as to which one of the measurements yielded the incorrect values. Therefore, for the experiments performed in phase three, as shown in appendix A, air values were also measured by the Gravimetric method. In this way, it was possible to have a three way check on the measured values.

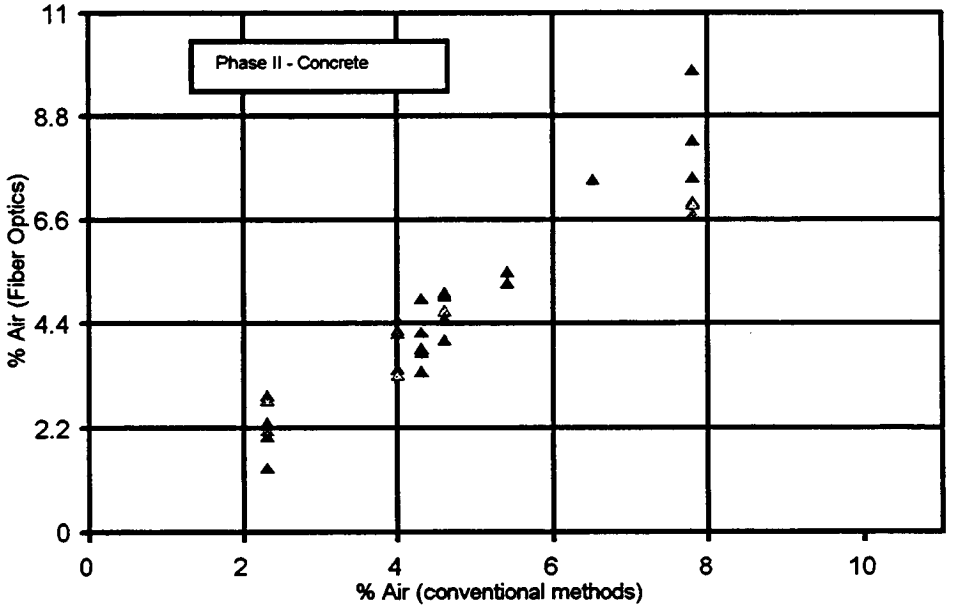

Fig. 35 Comparison of Fiber Optic measurements with conventional methods (Concrete).

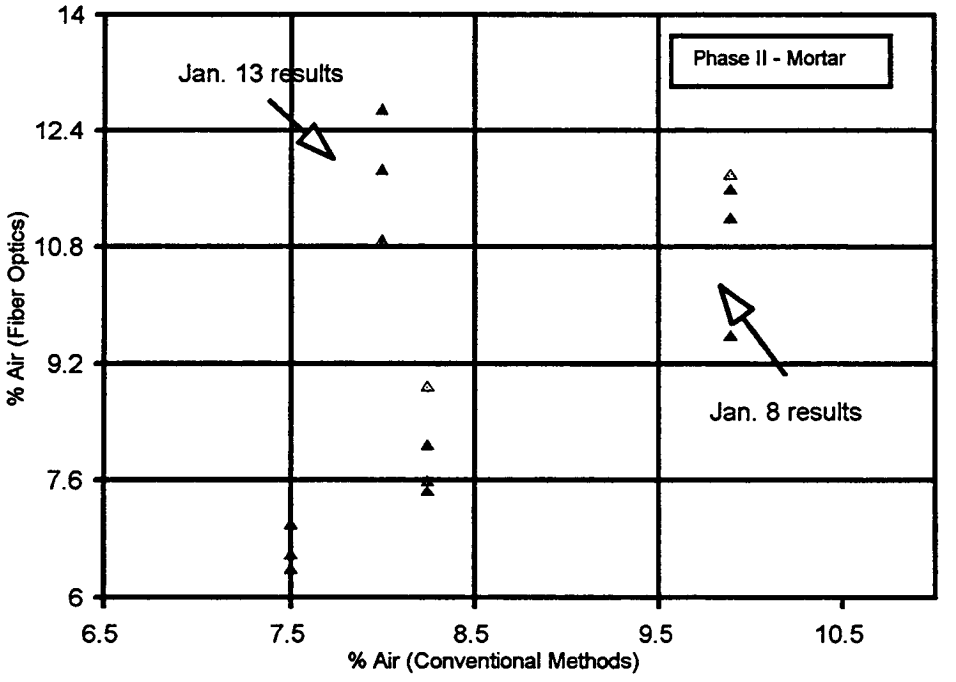

Fig. 36 Comparison of Fiber Optic measurements with conventional methods (Mortar).

Experimental results shown in Fig. 37 pertain to the measurement of air in concrete during phase 3 of the project (table 3). In these series of experiments, it was possible to produce concretes with relatively higher values of air. During this phase of the project, a three way check was made on the measurements using the pressuremeter, the optical fiber, and the Gravimetric method. As depicted in Fig. 37, the measurements taken by the three methods agreed relatively well for five tests. For the experiment pertaining to the very high air concrete (March 9, 1993 experiments), the pressuremeter readings were much larger than the values obtained by the Gravimetric, and Fiber Optic methods. This can be clearly observed by comparing the presuremeter measured value of 22 percent against the fiber optic scanned values of 14.21, 15.20, and the gravimetric measurement of 16.88 percent respectively. A number of possibilities may have caused the disagreement between the pressuremeter reading and the others. For instance, the fiber optic sensor was damaged after two

readings. Therefore, it is quite conceivable that the air values obtained through fiber optic scans have yielded erroneous results. Air contents calculated by the Gravimetric method are highly dependent on the specific gravities of the constituents, especially with regards to the aggregates. Hence, our testing procedure included repeated measurement of the specific gravities during the course of the experiments. Error during any one of the measurement steps would result in wrong air values.

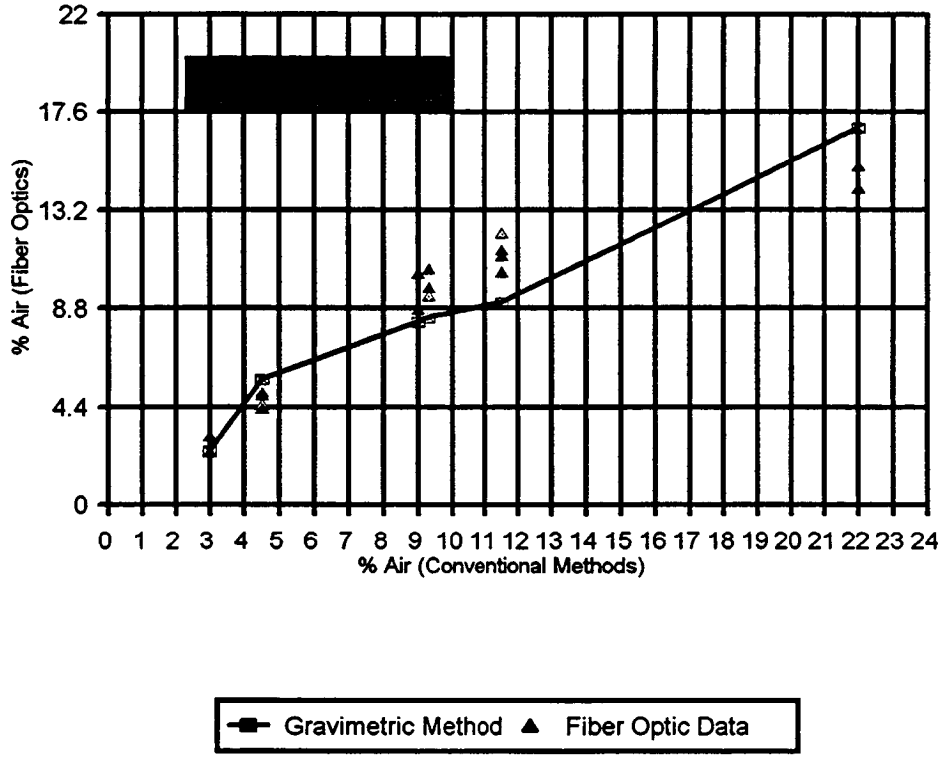

Fig. 37 Comparison of Fiber Optic measurements with conventional methods (Concrete).

Another important element of phase three experiments is associated with measurments of air in mortars sieved from concretes. These mortars were extracted from the concretes whose air contents were measured earlier (Fig. 37). Sieved mortar air values are presented in Fig. 38. Air values in sieved mortars should be higher than the concretes they are sieved from. This is due to the fact that in the new matrix, aggregates are replaced with mortars. Therefore, all the sieved samples, should reflect the increase in air content. Hence, this provided us with another check on the experimental results. In particular, examination of table 3 for the very high air content concrete (March 9,1993) reveals that the pressuremeter yielded an air content of 17 percent for the sieved mortar. This value is 5 % lower than the pressuremeter

value obtained from the same concrete (22%) from which the mortar was sieved from. Examination of table 3 further reveals that, as expected, the measured air values for all the other sieved mortars were larger than the concretes out of which they were extracted from. At this point, we are very sure that either human error, or the pressuremeter malfunction was responsible for the high air value recorded for the concrete of March 9 experiments.

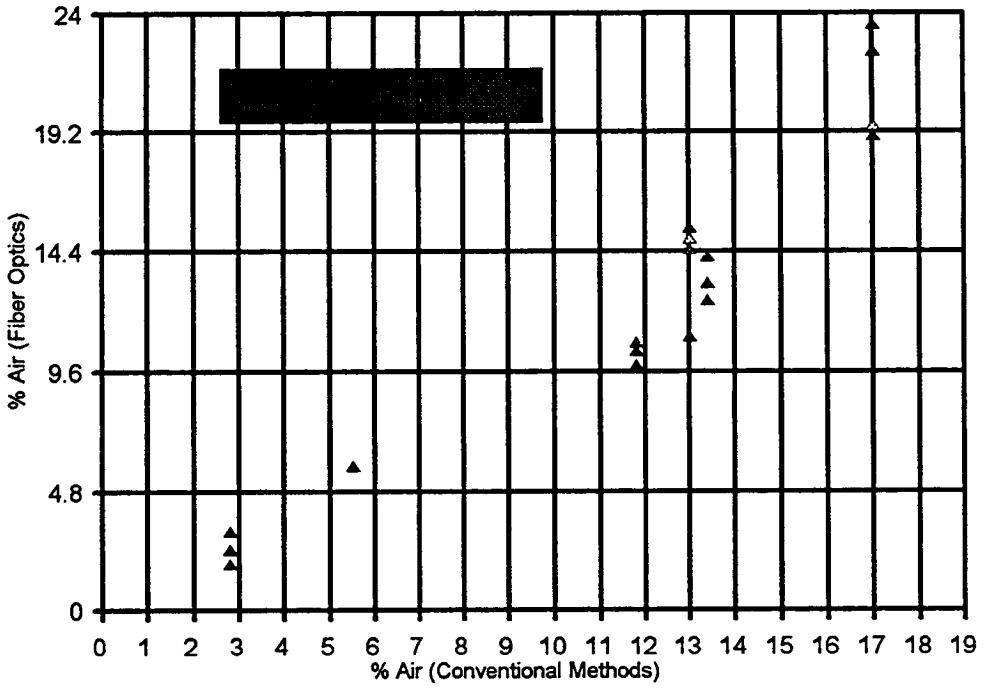

Fig. 38 Comparison of Fiber Optic measurements with conventional methods (Sieved Mortar).

Fig. 39 represents the combined experimental results for all the samples tested in phases 2 and 3 of this project (mortar and concrete). As this figure depicts, for all practical purposes, fiber optic and conventional method results present a good degree of correlation. In some cases, the fiber optic results proved to be more reliable than the pressuremeter. However, fiber optic data also indicated a rather large scatter. In some instances, the scatter was translated to a 2% air difference for measurements taken within the same concrete.

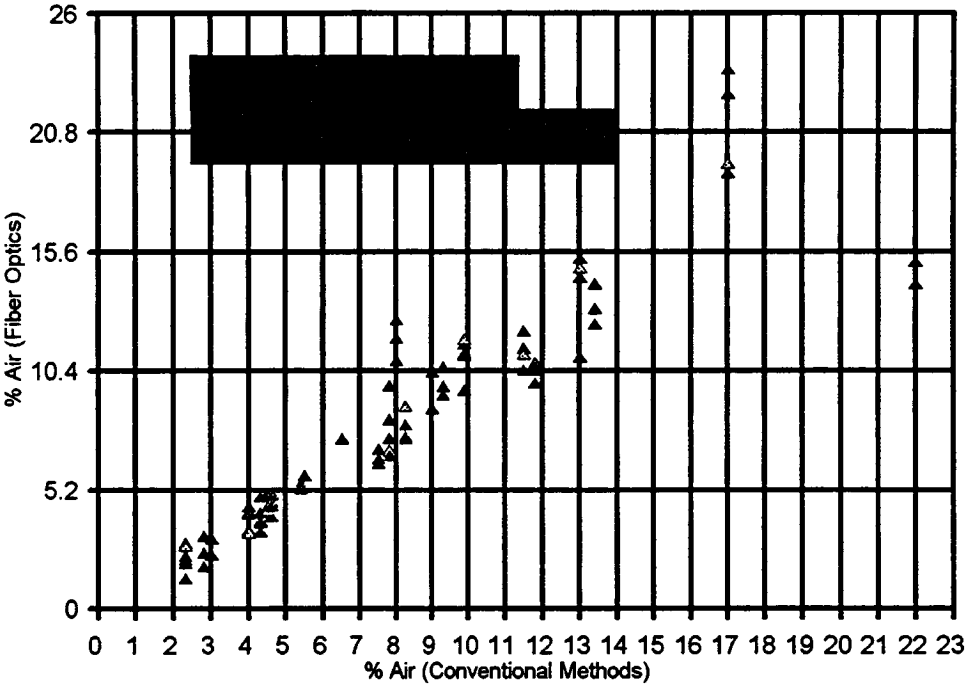

Fig. 39 Comparison of Fiber Optic measurements with conventional methods (combined experiments).

Conclusions and Recommendations

The primary objective of the work reported herein was to perform a series of experiments in order to verify the capability of the fiber optic sensor in detection of air bubbles in fresh concrete matrix. Development of a hardened probe tip for field applications was an equally important objective of this project, and it was implemented in parallel with the verification experiments. The experimental results have verified the effectiveness of the Fiber Optic sensor in measuring the amount of air in concrete. These results are very encouraging, since all the experimental results were obtained by using Plain-tipped sensors. In other words, a slight improvement in manufacturing process resulted in longer lasting sensors. We did not employ an aggregate repelling device with these sensors. This greatly improved our

experimental results, since the aggregate repelling devices slow down the flow of mortar across the tip. Neverthless, the concretes tested in the present study hardly resemble the ones mixed for use in highway pavements. Our experiments indicated that these sensors are not ready for use with highway mixes.

As our tabulated results indicate, it was not possible to come up with equal number of fiber optic scans for all the experiments. Fiber Optic scans lasted as long as the sensors remained in good condition. A sensor which lasted for six or seven times in one experiment, would usually fail after one or two trials in another set of tests. It seems that scatter of fiber optic data for measurements within the same concrete may be attributed to gradual accumulation of damage , and or scratches at the sensor tip.

As it was previously mentioned, it was not possible to employ the diamond disk probe heads because of the bond failure at the fiber to diamond wafer interface. Our search for a solution to this problem has led us to come across a new technology which is currently in practical use for protecting the lifetime of materials against erosion from high-speed particles and droplets. This technology which is available through SI Diamond Technology, Inc. consists of using a pulsed laser for heating a graphite feedstock in a low-pressure, ultra-high vaccum system. As the laser heats the graphite, it creates a plasma vapor that contains energetic carbon ions. When the carbon ions settle on the fiber optic tip, they produce diamond films called Amorphic Diamond. Because this process is performed at relatively low temperatures (about 35 degrees C), it will not damage the optical fiber. Amorphic Diamond coating is less brittle than crystalline diamond, and bond better to the fiber because it has less internal stress. A coating thickness of five microns is sufficient to protect the fiber tip from the harsh concrete environment.

Based on the foregoing discussion, it is recommended that to pursue this work one step further before its practical implementation in the field. The work should involve employment of the above-mentioned technology in hardening the probe tip. This work should also involve a verification step through a similar set of experiments as reported in the present work.

Appendix

Experimental data from February 12, 1993 fresh concrete tests

MIX DESIGN:
by weight:
Cement = 1
Sand = 2.24
Gravel = 2.10
Water = 0.55

mix proportion to produce 0.75 cubic feet of concrete:

cem := 17.18 pounds
ws := 39.00 pounds
wa := 36.00 pounds
wat := 9.45 pounds
wb := 0.315 pounds (MBVR-air entraining agent)

Wt := cem + ws + wa + wat + wb Wt = 101.945 Pounds

C-138 GRAVIMETRIC METHOD FOR MEASURING AIR CONTENT
VOLUME OF THE PRESSURE METER IS USED AS REFERENCE:

Wconc := 31.855 weight of mixed concrete in pressuremeter (pounds)

Vconc := 0.25 cubic feet, volume of concrete in pressure meter

$\gamma conc := \frac{Wconc}{Vconc}$ $\gamma conc = 127.42$ measured unit weight of concrete

$Vm := \frac{Wt}{\gamma conc}$ Vm = 0.8001 measured volume of concrete based on original 0.75 cubic feet mix design (cubic feet)

calculate the volume of each individual ingredient based on the measured weights:

ρw := 62.4 pounds/cubic feet

SGC := 3.15 Specific Gravity of Cement

SGS := 2.358 Specific Gravity of Sand (measured value)

SGA := 2.6 Specific Gravity of Aggregate (measured value)

$va := \frac{wa}{SGA \cdot \rho w}$ va = 0.2219 cubic feet

$vc := \frac{cem}{SGC \cdot \rho w}$ vc = 0.0874 cubic feet

$vs := \frac{ws}{SGS \cdot \rho w}$ vs = 0.2651 cubic feet

vw := .1514 measured directly (cubic feet)

vb := 0.007064 measured volume of MBVR (cubic feet)

Vt := vc + vs + va + vw + vb Vt = 0.7328 cubic feet

$Acongrav\% := \left(\frac{Vm - Vt}{Vm}\right) \cdot 100$ Acongrav% = 8.4061

Aconpres% := 9.3

MEAURED AIR CONTENT BY THE PRESSUREMETER FOR CONCRETE (Aconpres%) = 9.3%

Concrete was then seived, the air content of mortar obtained in this way was then measured by the fiber optic method. Since there were not enough material left for pressuremeter, the air content of the seived mortar was obtained by the Roll-A-Meter.

MEASURED AIR CONTENT OF MORTAR FOR SEIVED MORTAR BY ROLL-A-METER=13.4%
Amorol% := 13.4

SUMMARY

Acongrav% = 8.4061

Aconpres% = 9.3

Amorol% = 13.4

Experimental data from February 19, 1993 fresh concrete tests

MIX DESIGN: program mixdes.mcd was employed in coming up with the following mix.
by weight:
Cement = 1
Sand = 2.27
Gravel = 2.10
Water = 0.55

mix proportion to produce 1.0 cubic feet of concrete:

cem := 22.9 Cement (pounds)
ws := 52.0 Sand (pounds)
wa := 48.0 Aggregate (pounds)
wat := 12.6 Water (pounds)
wb := 1.01 MBVR, Air Entraining Agent (pounds)

$Wt := cem + ws + wa + wat + wb$ $Wt = 136.51$ cubic feet

C-138 GRAVIMETRIC METHOD FOR MEASURING AIR CONTENT
VOLUME OF THE PRESSURE METER IS USED AS REFERENCE:

Wconc := 32.55 weight of mixed concrete in pressuremeter (pounds)

Vconc := 0.25 cubic feet, volume of concrete in pressure meter

$\gamma conc := \frac{Wconc}{Vconc}$ $\gamma conc = 130.2$ measured unit weight of concrete

$Vm := \frac{Wt}{\gamma conc}$ $Vm = 1.048$ measured volume of concrete based on original 0.75 cubic feet mix design (cubic feet)

calculate the volume of each individual ingredient based on the measured weights:

ρw := 62.4 pounds/cubic feet

SGC := 3.15 Specific Gravity of Cement

SGS := 2.5135 Specific Gravity of Sand (measured value)

SGA := 2.669 Specific Gravity of Aggregate (measured value)

$va := \frac{wa}{SGA \cdot \rho w}$ $va = 0.288$ cubic feet

$vc := \frac{cem}{SGC \cdot \rho w}$ $vc = 0.117$ cubic feet

$vs := \frac{ws}{SGS \cdot \rho w}$ $vs = 0.332$ cubic feet

vw := 0.201923 measured directly (cubic feet)

vb := 0.01766 measured volume of MBVR (cubic feet)

$Vt := vc + vs + va + vw + vb$ $Vt = 0.956$ cubic feet

$Acongrav\% := \left(\frac{Vm - Vt}{Vm}\right) \cdot 100$ $Acongrav\% = 8.834$

Aconpres% := 9.0

Measured Air Content of Sieved Mortar By Pressuremeter= Amorpres% := 11.8

SUMMARY

Acongrav% = 8.834

Aconpres% = 9 Amorpres% = 11.8

Experimental data from March 9, 1993 fresh concrete tests

MIX DESIGN:
by weight:
Cement = 1
Sand = 3.1
Gravel = 1.35
Water = 0.60

mix proportion to produce 0.75 cubic feet of concrete:

cem := 22.22	Cement (pounds)
ws := 68.75	Sand (pounds)
wa := 30.00	Aggregate (pounds)
wat := 13.33	Water (pounds)
wb := 0.3150	MBVR, Air Entraining Agent (pounds)

Wt := cem + ws + wa + wat + wb Wt = 134.615 pounds

C-138 GRAVIMETRIC METHOD FOR MEASURING AIR CONTENT
VOLUME OF THE PRESSURE METER IS USED AS REFERENCE:

Wconc := 29.415 weight of mixed concrete in pressuremeter (pounds)

Vconc := 0.25 cubic feet, volume of concrete in pressure meter

$\gamma conc := \frac{Wconc}{Vconc}$ γconc = 117.66 measured unit weight of concrete

$Vm := \frac{Wt}{\gamma conc}$ Vm = 1.144 measured volume of concrete based on original 0.75 cubic feet mix design (cubic feet)

calculate the volume of each individual ingredient based on the measured weights:

ρw := 62.4 pounds/cubic feet

SGC := 3.15 Specific Gravity of Cement

SGS := 2.51 Specific Gravity of Sand (measured value)

SGA := 2.67 Specific Gravity of Aggregate (measured value)

$va := \frac{wa}{SGA \cdot \rho w}$ va = 0.18 cubic feet

$vc := \frac{cem}{SGC \cdot \rho w}$ vc = 0.113 cubic feet

$vs := \frac{ws}{SGS \cdot \rho w}$ vs = 0.439 cubic feet

vw := 0.2136 measured directly (cubic feet)

vb := 0.005298 measured volume of MBVR (cubic feet)

Vt := vc + vs + va + vw + vb Vt = 0.951 cubic feet

$Acongrav\% := \left(\frac{Vm - Vt}{Vm}\right) \cdot 100$ Acongrav% = 16.882

Aconpres% := 22

Measured Air Content of Sieved Mortar By Pressuremeter= Amorpres% := 17.0

SUMMARY

Acongrav% = 16.882

Aconpres% = 22 Amorpres% = 17

Experimental data from march 23, 1993 fresh concrete tests

MIX DESIGN:
by weight:
Cement = 1
Sand = 2.24
Gravel = 2.10
Water = 0.58

mix proportion to produce 1.0 cubic feet of concrete:

cem := 22.9 Cement (pounds)
ws := 51.4 Sand (pounds)
wa := 48.0 Aggregate (pounds)
wat := 13.3 Water (pounds)
wb := 0.0 MBVR, Air Entraining Agent (pounds)

$Wt := cem + ws + wa + wat + wb$ Wt = 135.6 pounds

C-138 GRAVIMETRIC METHOD FOR MEASURING AIR CONTENT
VOLUME OF THE PRESSURE METER IS USED AS REFERENCE:

Wconc := 34.955 weight of mixed concrete in pressuremeter (pounds)

Vconc := 0.25 cubic feet, volume of concrete in pressure meter

$\gamma conc := \frac{Wconc}{Vconc}$ $\gamma conc = 139.82$ measured unit weight of concrete

$Vm := \frac{Wt}{\gamma conc}$ Vm = 0.97 measured volume of concrete based on original 0.75 cubic feet mix design (cubic feet)

calculate the volume of each individual ingredient based on the measured weights:

$\rho w := 62.4$ pounds/cubic feet

SGC := 3.15 Specific Gravity of Cement

SGS := 2.51 Specific Gravity of Sand (measured value)

SGA := 2.67 Specific Gravity of Aggregate (measured value)

$va := \frac{wa}{SGA \cdot \rho w}$ va = 0.288 cubic feet

$vc := \frac{cem}{SGC \cdot \rho w}$ vc = 0.117 cubic feet

$vs := \frac{ws}{SGS \cdot \rho w}$ vs = 0.328 cubic feet

vw := 0.2136 measured directly (cubic feet)

vb := 0 measured volume of MBVR (cubic feet)

$Vt := vc + vs + va + vw + vb$ Vt = 0.946 cubic feet

$Acongrav\% := \left(\frac{Vm - Vt}{Vm}\right) \cdot 100$ Acongrav% = 2.417

Aconpres% := 3

Measured Air Content of Sieved Mortar By Pressuremeter= Amorrol% := 2.8

SUMMARY

Acongrav% = 2.417

Aconpres% = 3 Amorrol% = 2.8

Experimental data from April 5, 1993 fresh concrete tests

MIX DESIGN:
by weight:
Cement = 1
Sand = 2.3
Gravel = 2.1
Water = 0.60

mix proportion to produce 1.0 cubic feet of concrete:

cem := 22.22 Cement (pounds)

ws := 51.4 Sand (pounds)

wa := 48.0 Aggregate (pounds)

wat := 13.33 Water (pounds)

wb := 1.04 pounds (MBVR, air-entraining agent)

$Wt := cem + ws + wa + wat + wb$

$Wt = 134.99$ pounds

C-138 GRAVIMETRIC METHOD FOR MEASURING AIR CONTENT
VOLUME OF THE PRESSURE METER IS USED AS REFERENCE:

Wconc := 32.505 weight of mixed concrete in pressuremeter (pounds)

Vconc := 0.25 cubic feet, volume of concrete in pressure meter

$\gamma conc := \frac{Wconc}{Vconc}$ $\gamma conc = 130.02$ measured unit weight of concrete

$Vm := \frac{Wt}{\gamma conc}$ $Vm = 1.0382$ measured volume of concrete based on original 1.0 cubic feet mix design (cubic feet)

calculate the volume of each individual ingredient based on the measured weights:

$\rho w := 62.4$ pounds/cubic feet

SGC := 3.15 Specific Gravity of Cement

SGS := 2.51 Specific Gravity of Sand (measured value)

SGA := 2.67 Specific Gravity of Aggregate(measured value)

$va := \frac{wa}{SGA \cdot \rho w}$ $va = 0.2881$ cubic feet

$vc := \frac{cem}{SGC \cdot \rho w}$ $vc = 0.113$ cubic feet

$vs := \frac{ws}{SGS \cdot \rho w}$ $vs = 0.3282$ cubic feet

$vw := 0.2136$ measured volume of water (cubic feet)

$vb := 0.00106$ measured volume of MBVR (cubic feet)

$Vt := vc + vs + va + vw + vb$ $Vt = 0.944$ cubic feet

$Acongrav\% := \left(\frac{Vm - Vt}{Vm}\right) \cdot 100$ $Acongrav\% = 9.0775$ Air content of concrete (Gravimetric)

$Aconpres\% := 11.5$

MEASURED AIR CONTENT OF SEIVED MORTAR BY ROLL-A-METER $Amorroll\% := 13$

SUMMARY

$Acongrav\% = 9.0775$

$Aconpres\% = 11.5$

$Amorroll\% = 13$

Experimental data from April 7, 1993 fresh concrete tests

MIX DESIGN:
by weight:
Cement = 1
Sand = 2.3
Gravel = 2.1
Water = 0.60

mix proportion to produce 1.0 cubic feet of concrete:

cem := 22.22 Cement (pounds)

ws := 51.4 Sand (pounds)

wa := 48.0 Aggregate (pounds)

wat := 13.33 Water (pounds)

wb := 1.01 pounds (MBVR, air-entraining agent)

$Wt := cem + ws + wa + wat + wb$

Wt = 134.96 pounds

C-138 GRAVIMETRIC METHOD FOR MEASURING AIR CONTENT
VOLUME OF THE PRESSURE METER IS USED AS REFERENCE:

Wconc := 33.74 weight of mixed concrete in pressuremeter (pounds)

Vconc := 0.25 cubic feet, volume of concrete in pressure meter

$\gamma conc := \frac{Wconc}{Vconc}$ $\gamma conc = 134.96$ measured unit weight of concrete

$Vm := \frac{Wt}{\gamma conc}$ Vm = 1 measured volume of concrete based on original 1.0 cubic feet mix design (cubic feet)

calculate the volume of each individual ingredient based on the measured weights:

ρw := 62.4 pounds/cubic feet

SGC := 3.15 Specific Gravity of Cement

SGS := 2.51 Specific Gravity of Sand (measured value)

SGA := 2.67 Specific Gravity of Aggregate(measured value)

$va := \frac{wa}{SGA \cdot \rho w}$ va = 0.2881 cubic feet

$vc := \frac{cem}{SGC \cdot \rho w}$ vc = 0.113 cubic feet

$vs := \frac{ws}{SGS \cdot \rho w}$ vs = 0.3282 cubic feet

$vw := 0.2136$ measured volume of water (cubic feet)

$vb := 0.000353$ measured volume of MBVR (cubic feet)

$Vt := vc + vs + va + vw + vb$ $Vt = 0.9433$ cubic feet

$Acongrav\% := \left(\frac{Vm - Vt}{Vm}\right) \cdot 100$ $Acongrav\% = 5.6727$ Air content of concrete (Gravimetric)

$Aconpres\% := 4.5$

MEAURED AIR CONTENT BY THE PRESSUREMETER FOR CONCRETE=4.5%

MEASURED AIR CONTENT OF SEIVED MORTAR BY ROLL-A-METER=$Amorroll\% := 5.5$

SUMMARY

$Acongrav\% = 5.6727$ $Aconpres\% = 4.5$

$Amorroll\% = 5.5$